Microalgae-based bioremediation of olive mill wastewater: Technical and environmental evaluations using orange peel and orange peel-derived biochar

Sustainable Materials and Technologies 43 (2025) e01338

Contents lists available at ScienceDirect

Sustainable Materials and Technologies

journal homepage: www.elsevier.com/locate/susmat

Microalgae-based bioremediation of olive mill wastewater: Technical and environmental evaluations using orange peel and orange peel-derived biochar

Martina Lenzuni [a,b,c], Francesca Demichelis [b,d,*], Juan Felipe Basbus [a], Antonio Barbucci [a], Francesco Savorani [b,d], Tonia Tommasi [b,d], Alessandro Alberto Casazza [a,b]

[a] Department of Civil, Chemical, and Environmental Engineering (DICCA), University of Genoa (UniGe), Genoa, Italy
[b] National Research Centre for Agricultural Technologies (CN AgriTech), Naples, Italy
[c] Institute of Electronics, Computer and Telecommunication Engineering (IEIIT), National Research Council (CNR), Milan, Italy
[d] Department of Applied Science and Technology (DISAT), Polytechnic of Turin (PoliTo), Turin, Italy

ARTICLE INFO

Keywords:
Microalgae immobilization
Cell-material interactions
Agro-industrial waste
Bioremediation
Pyrolysis
Environmental evaluation

ABSTRACT

The discharge of olive mill wastewater (OMWW) presents significant environmental challenges due to its high pollutant load, necessitating sustainable management solutions. This study explores a novel approach to treat OMWW through microalgae-based bioremediation using orange peel (OP) and OP-derived biochar as matrices for microalgae immobilization. Aligning with the principle of bioeconomy, this study treats a waste (OMWW) with another waste in its raw form and as a high-value-added product maximizing its potential (OP and OP-derived biochar). The technical feasibility and the environmental footprint through Life Cycle Assessment (LCA) are evaluated. LCA includes different impact categories and focuses on climate change to quantify decarbonization, considering as a function unit (FU) 10 g of OP (the amount used in the bioremediation tests). OMWW was explored at 5 % and 10 % *v*/v (according to literature studies) using *Chlorella vulgaris* immobilized on OP (scenario 1) and OP-derived biochar (scenario 2) of the chosen size. Scenario 1 (OMWW at 10 % *v*/v) reached the highest performance by achieving ~70 % phenolic compound degradation, ~ 60 % chemical oxygen demand abatement, and a climate change impact of 0.43 kg $CO_{2\ eq}$/FU. The strengths of Scenario 1 include high bioremediation capacity and energy recovery from pyrolyzing microalgae-immobilized exhausted OP, specifically refining pyrolysis bio-oil as an energy carrier which generates a surplus of energy. These results demonstrate the potential of integrating microalgae with waste substrates for environmental remediation and energy recovery, offering a sustainable approach to mitigate disposal impacts and close the loop in agro-industrial systems.

1. Introduction

Waste disposal is a pressing global challenge, particularly in regions where intensive agricultural activity generates significant amounts of organic waste. Among these, the Mediterranean area is notable for its extensive production of citrus fruits and olives, leading to substantial quantities of orange peel (OP) and olive mill wastewater (OMWW). The disposal of these organic wastes presents environmental, economic, and social challenges, including pollution, greenhouse gas emissions, and resource wastage [1]. In particular, aqueous effluents from olive oil industries (~0.5 m^3 per 1000 kg of processed olives) contain several contaminants and high amounts of phenolic compounds (over 6 g/L), and the discharge of these into water bodies and open spaces without treatment is reported to impact on the environment [2,3]. It has been also reported that, in terms of pollution effect, 1 m^3 of OMWW is equivalent to 100–200 m^3 of domestic sewage, highlighting its substantial pollution potential [4]. Despite these challenges, such waste streams may also offer unique opportunities for valorization within a circular bioeconomy framework.

Microalgae-based biodegradation provides an affordable and environmentally friendly alternative to chemical or physical pollutant removal processes. This approach not only treats wastewater but also

* Corresponding author at: National Research Centre for Agricultural Technologies (CN AgriTech), Naples, Italy.
E-mail address: francesca.demichelis@polito.it (F. Demichelis).

https://doi.org/10.1016/j.susmat.2025.e01338
Received 25 November 2024; Received in revised form 19 January 2025; Accepted 28 February 2025
Available online 2 March 2025

produces valuable biomass, making it increasingly attractive [5]. However, a persistent challenge with microalgal treatment is the harvesting of algal cells, which limits the efficiency and scalability of these systems. To overcome this limitation, the immobilization of microalgae onto solid supports has been explored as a promising approach, allowing for more efficient biomass recovery and potentially enhancing the stability of the treatment system. Further, functional groups from the immobilized substrate can participate in the bioremediation process. While immobilized living microalgae have been used for the removal of single inorganic nutrients (e.g., ammonium, nitrate, and phosphate) and heavy metals, research on their application for the degradation of toxic organic pollutants, specifically from agricultural effluents like OMWW, remains sparse [6]. Additionally, there is currently no published information on using OP as a matrix for immobilizing microalgae for such applications. Several synthetic carriers such as porous glass, ceramics, polyurethane foam, and polyvinylidene fluoride, have been successfully used for microalgal immobilization [7]. However, natural biomass-based scaffold materials are less commonly used. These typically include loofah [8], corn cob [9], or pine bark [10]. Furthermore, microalgae can be immobilized on a natural biomass as it is or on the solid product of the pyrolysis, named biochar. The immobilization of microalgae on biochar is a topic of growing interest in environmental and biotechnological research due to its potential applications in wastewater treatment for the removal of heavy metals and environmental mitigation [11,12]. This integrated approach not only opens new routes for the bioremediation of phenolic-rich effluents but also leverages agricultural waste within a circular bioeconomy framework, offering a model that could be adapted for similar waste types globally.

Moreover, this work integrates environmental assessment through ex-ante Life Cycle Assessment (LCA), a tool rarely applied to emerging bioremediation technologies. In fact, after proving technical feasibility, the environmental impact of these strategies must be assessed to enable future scale-up. For this scope, the worldwide adopted tool is the LCA, performed according to the International Organization for Standardization (ISO) 14040–44 standards. Conventional LCA studies typically focus on established market-implemented plants and technologies, whereas emerging technologies like bioremediation with immobilized microalgae present challenges. These are derived from their low technological readiness level, which leads to uncertainties in scaling up and, consequently, uncertainties in the quantification of the ecological effects [13]. To face these challenges, the LCA community provides early support to technology developers through quantitative tools and by performing “ex-ante” LCA using the data obtained at the laboratory scale [14].

Overall, this study investigated the technical feasibility and the environmental impacts of the bioremediation of OMWW with immobilized microalgae on OP and OP-derived biochar. By combining technical feasibility analysis with environmental impact assessment, this work pioneers a sustainable waste management strategy with the potential for broader application and scale-up. This study is the first to explore the synergistic valorization of OP and OMWW by utilizing OP-based matrices for the immobilization of microalgae in a bioremediation system. By addressing the gap in sustainable disposal methods for these wastes and evaluating environmental effects through ex-ante LCA, this study lays the groundwork for future innovations in circular bioeconomy solutions and resource-efficient waste management.

2. Materials and methods

2.1. Materials

The microalgal strain used in the experiments was *Chlorella vulgaris* CCAP 211, which was obtained from the Culture Collection of Algae and Protozoa (Argyll, UK). The raw olive mill wastewater (OMWW) has been supplied by a three-phase mill in Tuscany (Italy). OMWW has been centrifuged at 5000 $\times g$ for 5 min to separate the liquid phase (subsequently used for the bioremediation experiments) from the solid residues. Fresh orange peel (OP) was sourced from the local market in Italy and immediately washed with distilled water to remove impurities. All the materials and samples were stored in a freezer at −20 °C until use. Upon removal from the freezer, the orange peels and OMWW samples were allowed to thaw gradually at room temperature to minimize any potential thermal shock that could alter their structure or chemical composition. Calcium chloride ($CaCl_2$), magnesium sulphate ($MgSO_4$), monopotassium phosphate (KH_2PO_4), iron (III) chloride hexahydrate ($FeCl_3 \bullet 6H_2O$), sodium carbonate (Na_2CO_3), sodium chloride (NaCl), sodium nitrate ($NaNO_3$), and zinc chloride ($ZnCl_2$) were purchased from Carlo Erba Reagents (Milan, Italy). Vitamins B1, B8, and B12 were purchased from Thermo Fisher Scientific (Waltham, USA). Acetone, cobalt (II) chloride ($CoCl_2$), dipotassium hydrogen phosphate (K_2HPO_4), ethanol, ethylenedinitrilotetraacetic acid disodium salt dihydrate ($Na_2EDTA \bullet 2H_2O$), manganese (II) chloride tetrahydrate ($MnCl_2 \bullet 4H_2O$), Folin-Ciocalteu’s reagent, and sodium molybdate (Na_2MoO_4), were purchased from Sigma-Aldrich (St. Louis, MO, USA). Methanol, acetonitrile, and acetic acid (Carlo Erba Reagents, Milan, Italy) of analytical grade were used for high-performance liquid chromatography (HPLC).

2.2. Substrates characterization

OP and biochar samples (produced as explained in paragraph 2.5) were subjected to proximate analyses and ultimate analyses. Furthermore, the pH values of the samples were measured by mixing1 g of substrate in 20 mL of deionized water using a magnetic stirrer at 80 rpm for 2 h.

Before conducting the slow pyrolysis process, a thermogravimetric analysis (TGA) (using TGA/SDTA851, Mettler Toledo, Columbus, USA) was performed under an argon atmosphere (inert gas). This analysis aimed to determine the temperature range suitable for investigation, based on the capabilities of the fixed-bed pyrolysis reactor available in the laboratory (as detailed in paragraph 2.5). The temperature range assessed was from room temperature to 800 °C, with a heating rate of 10 °C/min.

Proximate analysis of samples was performed with the TGA instrument according to ASTM D7582–15. Briefly, 1 mg of a sample was heated from room temperature to 105 °C under argon for 30 min for the quantification of the moisture content. Then, the temperature was increased to 950 °C at 20 °C/min and kept constant for 7 min to quantify the content of volatile matter. Subsequently, the atmosphere changed from inert to oxidative, and the sample was combusted for 10 min to quantify the ash content. The fixed carbon (FC) content was determined as the difference in the percentage of moisture, volatile matter, and ash from 100 % (i.e., the total mass in percentage). Ultimate analysis concerning the elemental analysis (CHNS-O) was performed with a Vario Elementar Cube analyzer (Elementar, Hanau, Germany). A dry grounded sample (20 mg) was fed to the elemental analyzer to quantify the total carbon, hydrogen, nitrogen, and sulfur contents, while the oxygen content was calculated as a difference of these elements considering the ash content of the total sample mass. FTIR spectra of the samples were taken with a Fourier-transform infrared spectrophotometer (Nicolet iS50, Thermo Fisher Scientific Inc., WI, USA), and spectra were acquired in the 4000–500 cm^{-1} wavenumber range in the attenuated total reflectance (ATR) mode (ATR ID7/ITX, Thermo Fisher Scientific Inc., WI, USA). Samples morphologies were examined by scanning electron microscopy (SEM) using Phenom ProX desktop (Phenom-World BV, Eindhoven, Netherlands) operating at 10 kV with a secondary electron detector (SED). The samples were coated with a thin conductive layer by a gold sputtering machine.

Following established protocols from the literature, the main characteristics of both raw and centrifuged OMWW were determined [3]. These parameters include pH values of 5.25 and 5.29, chemical oxygen demand (COD) of 184.10 g_{O_2}/L and 88.65 g_{O_2}/L, total solids of 84.71 g/L

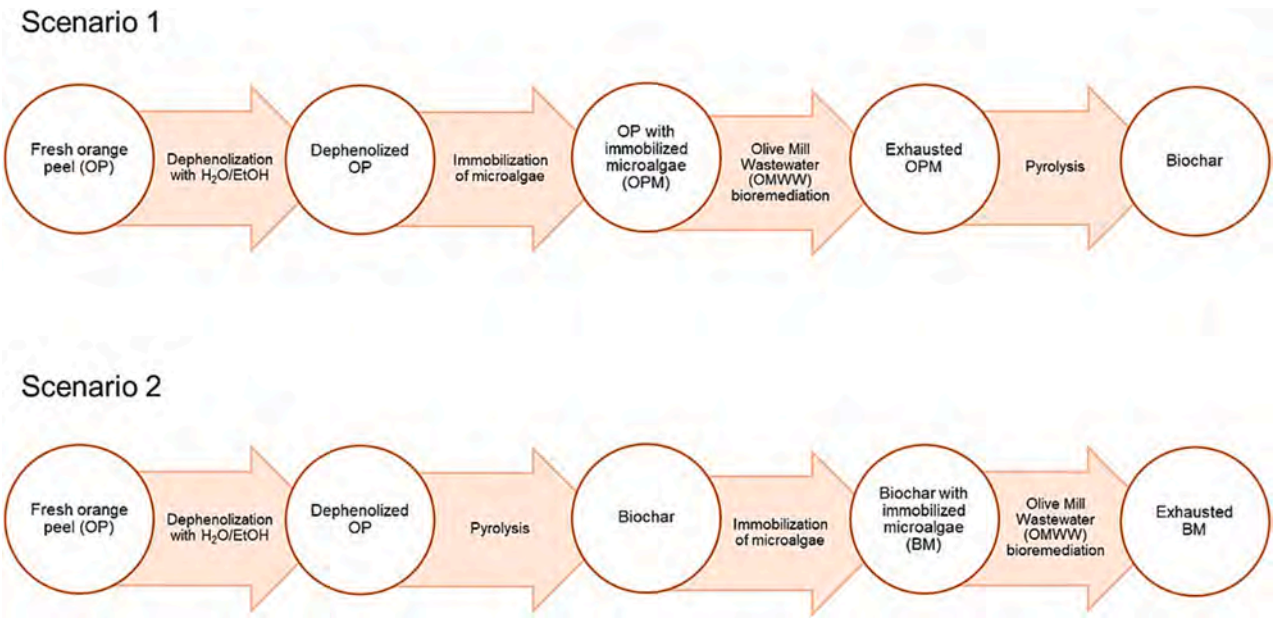

Fig. 1. Schematic diagram of the two proposed scenarios. In both cases, microalgae were immobilized on the chosen substrates (orange peel (OP) or OP-derived biochar) before the bioremediation assays with olive mill wastewater (OMWW).

and 25.19 g/L, and ash content of 1.33 % and 1.22 %, respectively.

2.3. Integrated strategies scenarios

Fig. 1 presents the diagrams of the evaluated integrated strategies scenarios for the OP valorization and OMWW treatment with microalgae. Scenario 1 comprised a first extraction of high-added value compounds (mainly polyphenols) from OP, followed by immobilization of microalgae on the dephenolized OP, bioremediation experiments with OMWW, and a final pyrolysis step to obtain biochar from the substrates. On the other hand, scenario 2 comprised a first pyrolytic step of the dephenolized OP, a subsequent immobilization of the microalgae on the obtained biochar, and a final bioremediation experiment with OMWW.

It must be noted that throughout the experiments performed, two distinct categories of phenolic compounds are under consideration. The first type of phenolic compounds is involved in an initial recovery step aimed at extracting "beneficial" polyphenols from orange peels. These recovered polyphenols have significant potential for future application in the pharmaceutical industry and as dietary supplements, where their antioxidant and health-promoting properties could be highly valuable [15,16]. In a later stage, the bioremediation analysis was focused on the uptake and biodegradation of phenolic compounds present in OMWW. Unlike the beneficial polyphenols from orange peels, the phenolic compounds in OMWW pose considerable environmental risks [2]. These compounds are particularly challenging to remove from OMWW and their purification and valorization are unfeasible. The degradation of these toxic phenols is therefore crucial in mitigating their harmful impact on the environment and in ensuring the safe disposal or reuse of treated wastewater.

2.4. Extraction of phenolic compounds from OP and subsequent HPLC analysis

As the first step of both scenarios, extraction of phenolic compounds from OP was carried out in a glass bottle, where 10.0 g of biomass were added to 100 mL of 70 % *v*/v ethanol aqueous solution and left under stirring at room temperature (25 ± 1 °C) for 16 h (i.e., overnight). The choice of solvent composition was derived from previous results obtained by our group and considering both ethanol and water as the greenest solvents available [17]. HPLC was subsequently used to qualitatively determine the extracted phenolic compounds from OP. To perform the analysis, 1 mL of filtered sample was centrifuged at 20,900 ×*g* for 15 min. An aliquot (700 µL) of the resulting supernatant was removed and 20 µL were injected in an HPLC Agilent 1260 Series system (Palo Alto, USA) combined with a diode array detector (DAD) using a C18 reverse-phase column (Eclipse plus, 250 mm × 4.6 mm id, 5 µm, Agilent, Santa-Clara, USA). The column was equilibrated with a mixture of solution A (MilliQ water containing 1 % *v*/v acetic acid) and B (50 % *v*/v methanol and 50 % *v*/v acetonitrile), and the solvent gradient was adjusted as reported in previous works [18]. The main detector wavelength was set at 280 nm. Identification of the compounds was determined by comparing their retention times and ultraviolet-visible (UV–Vis) spectra with those from the available literature and of standard solutions. Lastly, to enhance the rigidity and mechanical strength of dephenolized OP, a final hardening step of these substrates was performed by keeping them immersed in acetone at −20 °C for 30 min before washing them with deionized water [19].

2.5. Pyrolysis of OP and characterization of the resulting products

Slow pyrolysis was performed in a fixed-bed reactor at 400 °C at 10 °C/min with a residence time of 1 h. These operative parameters were selected based on thermogravimetric analysis (see paragraph 2.2) and on the works of Miranda et al. [20] who proved that around 300–400 °C, working with slow pyrolysis, there is the highest weight loss of the OP, and Selvarajoo et al. [21] who showed that 400 °C is a fair compromise between biochar yield, pyrolysis energy expenditure, and biochar physical properties (important for the adsorption and immobilization). The scheme and the technical information regarding the pyrolysis reactor are provided in previous literature [22]. Inert conditions were ensured by insufflating nitrogen at 500 mL/min measured through a mass flow rate controller. Solid, liquid, and gas phases were separately recovered. Approximately 10 g of biomass was manually fed into the pyrolysis reactor. The tested biomasses were the exhausted OP with immobilized microalgae at the end of the bioremediation process (scenario 1) and the fresh (dephenolized) OP (scenario 2). Before pyrolysis, the fresh and exhausted OP were dried at 105 °C for 24 h. The high heating value (HHV) of the bio-oil was measured through the IKA C7000 calorimetric bomb (IKA, Staufen, Germany).

Regarding scenario 2, fresh OP was initially cut and tested into three sizes: 0.5 cm × 0.5 cm, 1.0 cm × 1.0 cm, and 2.0 cm × 2.0 cm, to assess how the product distribution was correlated with the starting biomass dimension [23]. These sizes were selected based on the dimensions of the pyrolysis reactor and their suitability for handling during immobilization and bioremediation tests. The reactor was electrically heated in a stainless-steel chamber while the top of the reactor was connected to a jacketed condenser in which a coolant agent flowed. The condensable compounds were recovered in liquid form (oil + water), while non-condensable gases passed the condenser and were collected in a Tedlar gas bag. The gas phase was quantified by water displacement and qualitatively by micro gas chromatography (μCG) by Micro-GC Fusion equipment (INFICON, Bad Ragaz, Switzerland). At the end of pyrolysis, the reactor was cooled down and the biochar was manually recovered. The biochar yield was calculated as the ratio between the mass of the solid product of slow pyrolysis (g) and the dried OP mass (g). Characteristics of the resulting products were assessed as described in paragraph 2.2. A Brunauer-Emmett-Teller (BET) analyzer (Micromeritics TriStar II 3020 t) through the N_2 adsorption method measured the specific surface area (SSA) and pore volume of the grounded biochar. Before the BET analysis, the biochar was degassed under helium at 300 °C for 2 h. The biochar samples were then cooled in a liquid nitrogen bath at −196 °C for analysis. The morphology of the biochar was examined using a field-emission scanning electron microscope (FESEM S-4300, Hitachi, Tokyo, Japan) at an acceleration voltage of 3.0 kV after being coated under a vacuum with a thin layer of gold.

2.6. Microalgae growth and immobilization onto the substrates

Microalgae were grown in Bold's Basal Medium (BBM) [3] and cultivated at room temperature (25 ± 1 °C) under continuous illumination (70 μmol photons/(m^2*s), provided by 36 W fluorescent lamps (Rexer, Nanjing, China) on an orbital shaker (Innova 2100, VWR, Radnor, PA, USA) at 120 rpm. *C. vulgaris* growth behavior was assessed by optical density measurements using a spectrophotometer (Genova, Jenway, Stone, UK) set at 625 nm, and absorbance values were compared to a standard calibration curve to obtain dry biomass (g/L) values.

For the microalgae immobilization step of the two scenarios described in paragraph 2.3, dephenolized OP and OP-derived biochar substrates were incubated at room temperature (25 ± 1 °C) with a microalgae solution (0.7 g/L) in an orbital shaker at 120 rpm for 24 h under continuous illumination to allow sufficient attachment of microalgae cells to the substrates. Samples were then washed thoroughly with fresh BBM to remove any free microalgal cells.

2.7. Bioremediation studies

The desired concentrations of OMWW solutions (5 and 10 % *v*/v) were prepared by diluting the wastewater with tap water. These concentrations were selected based on previous studies with microalgae and OMWW, considering factors such as the dark color of the wastewater, the phenolic content, and the impact of different OMWW concentrations on the growth rate of microalgae in previous bioremediation processes [24–26]. The solutions were then incubated with microalgae-immobilized substrates, or substrates (OP or biochar) without microalgae over a contact period of 7 days. A negative control with only OMWW (5 and 10 % *v*/v) was included to isolate the contribution of photodegradation processes. A positive control with free microalgae and OMWW (5 and 10 % *v*/v) was added to evaluate the bioremediation capacity of the free microalgae in the absence of any immobilizing substrate. In the latter case, the initial concentration of microalgae (0.4 mg/mL and 0.2 mg/L) was derived after calculating the amount of microalgae attached on OP and biochar substrates before the start of the bioremediation experiments. Samples of treated OMWW were collected at set time intervals and filtered to determine the residual chemical oxygen demand (COD) (according to standard methods, such as ISO 15705:2002) and phenolic compounds concentrations by Folin-Ciocalteu assay (via UV–Vis spectrophotometry), as described in our previous works [17,18]. The morphologies of the substrates with attached microalgae at the end of the experiments were investigated by digital photos and by SEM, as described in paragraph 2.2. FTIR spectra of the same samples were also recorded as described in paragraph 2.2.

2.8. LCA and ex-ante environmental evaluation

The environmental analysis was conducted using SimaPro 9.5.0.2 software with the Ecoinvent 3.5 database. In this study, Life Cycle Assessment (LCA), conducted according to ISO 14040-44 (2006), was adopted as a recognized methodology to assess the environmental impacts of emerging technology systems. The aim of the analysis was the comparison of scenario 1 and scenario 2, considering the microalgae-based bioremediation of OMWW at 5 and 10 % *v*/v through fresh OP and OP-derived biochar. The objective was to identify the bioremediation process with the lowest environmental impact, thereby determining its feasibility for scaling from laboratory to pilot and eventually industrial scales. A functional unit (FU) of 10 g of OP, corresponding to the amount of biomass fed into the pyrolysis reactor, was selected, and a cradle-to-gate approach was adopted. The selected FU allowed a comparison between the investigated supports of the microalgae (fresh OP and OP-derived biochar) highlighting the environmental impacts associated with their different performances in the bioremediation of OMWW at 5 and 10 % *v*/v. Furthermore, the lab-scale value of FU was due to the performance of an LCA with an ex-ante approach, which was needed due to the novel and emerging nature of the processes under investigation, as they have not yet been tested at pilot or industrial scales. Consequently, predicting the potential variation in scale-up, productivity, and product quality was challenging. It must be noted that microalgae-based bioremediation utilizing by-products such as OP or valorized by-products like OP-derived biochar represents an innovative approach.

Life Cycle Inventory (LCI) was based on data derived from laboratory results described in paragraph 3.3 and reported in the Supplementary data (Tables S1, S2, S3, S4, and S5). The background and foreground systems were defined according to the literature [27], with the background system encompassing data like energy production and consumption and chemicals sourced from Ecoinvent 3.8.5. Since OP is a by-product, the zero-burden assumption was hypothesized, assuming no credits for impacts in prior lifecycle phases. The life cycle impact assessment was carried out considering the ReCiPe 2016 Midpoint (H) method, with a focus on the climate change impact category (kg CO_2 eq) to understand the gap between the emission of the bioremediation processes and the net zero emission trajectory (i.e. achieving carbon neutrality in 2050). A sensitivity analysis was carried out to prove the consistency of the environmental impact results obtained by varying the consideration of bio-oil. In detail, in the first environmental study, bio-oil was considered as a waste, while in the sensitivity analysis it was considered as an energy carrier, and its treatment was considered in terms of energy consumed to clean and separate it from the water phase.

2.9. Statistical analysis

All experiments were performed in triplicate. The standard deviation was represented in the error bars of each group. One-way analysis of variance (ANOVA) was applied for each experiment for a comparison of more than two group means. ANOVA analyses that gave significant differences were followed by a Bonferroni test for multiple comparisons to determine which conditions differed significantly. Three statistical significance values, indicated as * $p < 0.05$, ** $p < 0.01$ and *** $p < 0.001$, were considered.

Table 1
Physico-chemical characteristics of orange peel (OP). HHV corresponds to the higher heating value. The available literature studies about OP are reported for comparison.

Parameter	This work	Literature data
Moisture (%)	8.97 ± 2.72	6.18–13.00 [28–31]
Ashes (%)	3.55 ± 1.41	2.34–5.50 [28–31]
Volatile matter (%)	73.06 ± 5.73	50.90–70.80 [28–30,32]
Fixed carbon (%)	23.67 ± 6.98	19.56–34.80 [28–30,32]
C (%)	43.42 ± 4.22	40.3–47.00 [28–31]
H (%)	5.27 ± 0.62	4.83–6.00 [28–31]
N (%)	1.54 ± 0.03	0.50–1.56 [28–31]
S (%)	0.16 ± 0.02	0–0.27 [28–31]
O (%)	49.62 ± 4.65	45.00–52.90 [28–30]
pH	3.90 ± 1.03	nd
HHV (MJ/kg)	18.08 ± 0.99	16.83–18.28 [20,32]

3. Results and discussion

3.1. Characterization of the orange peel

The physico-chemical characterization of the orange peel (OP) is reported in Table 1, highlighting that OP consisted mainly of volatile matter and a small content of ashes. Comparable values were reported in the previous literature for similar samples [20,28–30]. The elemental composition of the OP analyzed in this study is consistent with that of OP reported in studies from other regions, confirming that the selected OP is a relevant and representative substrate.

The FTIR spectrum of dried OP is shown in Fig. 2 (b) while the list of band assignments is provided in Table S6. The spectrum presents the characteristic bands corresponding to cellulose, hemicellulose, and lignin, which are the main components of OP (around 70, 5, and 20 %, respectively), as reported in the literature [33,34]. In particular, the most intense band around 1020 cm^{-1} is associated with stretching of the link C-O-H and C-O-C of cellulose, lignin, and hemicellulose. The wide peaks around 3300 and 2900 cm^{-1} are due to the stretching vibration of the O—H and C—H bond, respectively. Other predominant peaks are observed at 1736 (C═O stretching of a carboxylic acid group in pectin and other polysaccharides), 1620 (C═C and C═O stretching), and 1279 (C—O stretching) cm^{-1}. The peak at 1430 cm^{-1} is associated with C—H bending vibrations, commonly found in methylene and methyl groups of lignocellulosic materials [35]. Finally, smaller peaks at 902, 809, and 745 cm^{-1} are associated with out-of-plane bending vibrations in cellulose and aromatic rings of phenolic structures [15,36,37]. Fig. 2 (c) represents the SEM image of the dephenolized OP and reveals a heterogeneous and porous "sponge-like" structure of the biomass with lots of cavities, as expected from previous studies in the literature [38,39]. These features, along with the chemical groups on the surface, are promising for adsorption of contaminants and microalgal cells. Lastly, the chromatogram of the ethanolic extract of OP is presented in Fig. 2 (d). The total phenolic content, expressed as milligrams of caffeic acid equivalents (CAE) per gram of OP, was 5 mg_{CAE}/g_{OP}. The compounds detected belong to different phenolic families, such as phenolic acids, flavonoids, flavonols, and flavones, with hesperidin and naringin being the most abundant compounds detected. Moreover, the spectrum shows the presence of several phenolic acids including *p*-coumaric, ferulic, and caffeic acid. These results confirmed that OP is a rich natural source of several phenolic compounds that are well-known for their antioxidant activities [16].

3.2. OP pyrolysis and characterization of biochar samples

A TGA was performed to analyze the composition of OP based on its

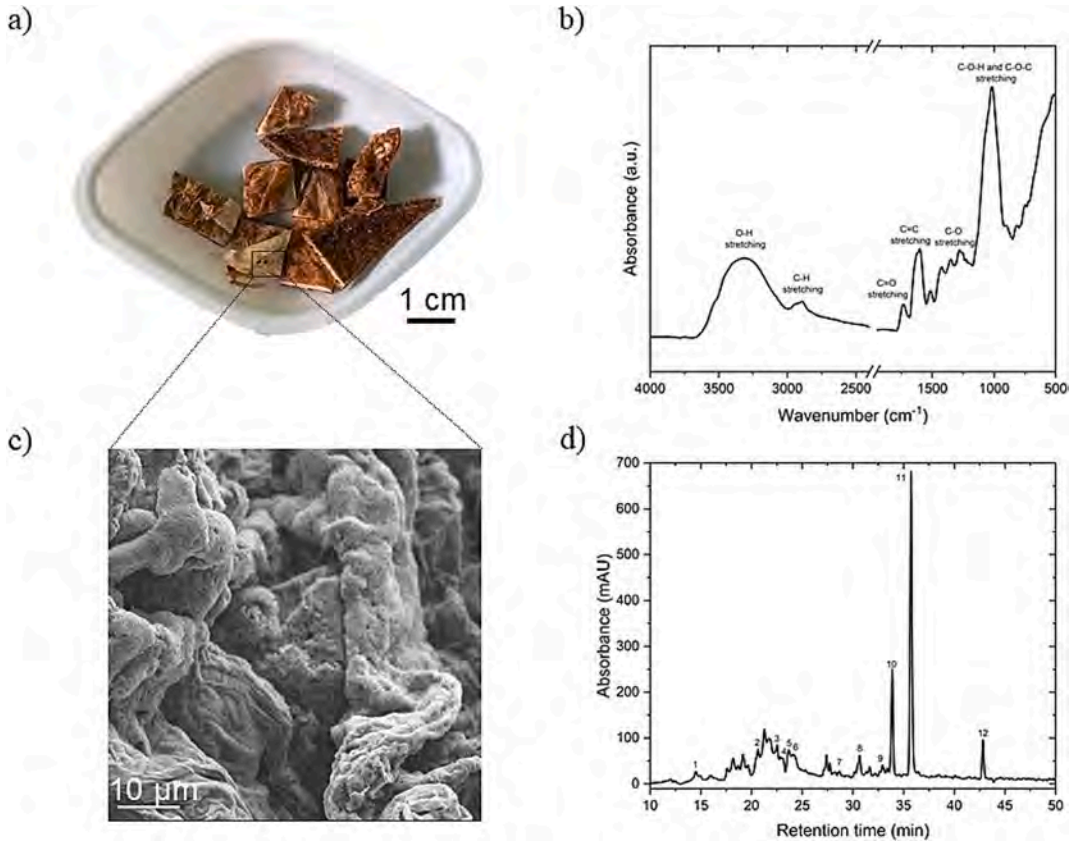

Fig. 2. Characterization of orange peel (OP). a) Digital photo of dried orange peel samples; b) FTIR spectrum and c) SEM image of OP. d) HPLC chromatogram of OP extract obtained from the solvent extraction step with ethanol (70 % *v*/v). HPLC peaks: 1, dihydroxybenzoic acid; 2, chlorogenic acid; 3, catechin; 4, vanillic acid; 5, caffeic acid; 6, siringic acid; 7, *p*-coumaric acid; 8, ferulic acid; 9, narirutin; 10, naringin; 11, hesperidin; 12, quercetin.

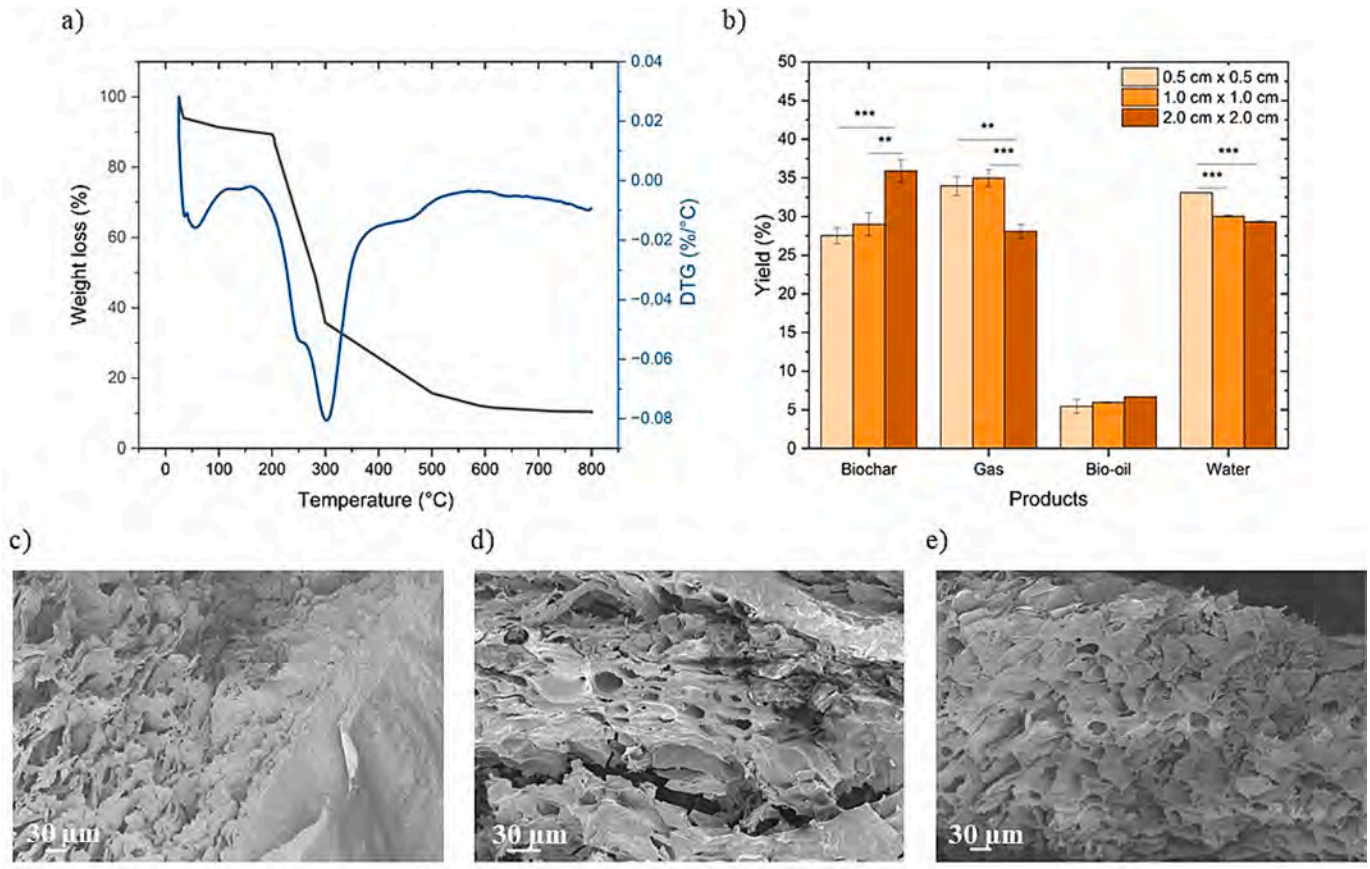

Fig. 3. a) TGA and DTG curves of orange peel (OP) investigated from room temperature to 800 °C under an inert atmosphere (argon). b) Product distribution from pyrolysis of OP samples of different piece sizes (** $p < 0.01$, *** $p < 0.001$). SEM images of biochar obtained from orange peel samples of size c) 0.5 × 0.5 cm^2, d) 1.0 × 1.0 cm^2, e) 2.0 × 2.0 cm^2. The visible biochar's porous structure facilitates microalgae immobilization by providing a high surface area for attachment.

thermal behavior, allowing the selection of an optimal temperature for the study's objective of using biochar to support microalgae immobilization. Considering the TGA and derivative thermogravimetry (DTG) results, OP can be considered as support mainly composed of hemicelluloses, followed by cellulose and lignin, since the highest loss of OP weight occurred between 220 and 300 °C, which is typical of hemicellulose, while the second significant loss of weight between 300 and 350 °C is usually associated with cellulose (Fig. 3 (a)). On the other hand, the decomposition of lignin occurs over a wide range of temperatures, usually between 200 and 800 °C, since lignin is a complex matter. It is of interest to note that the degradation of lignin allowed the development of meso- and micro-pores and increase of specific surface area, which are important parameters for the application of biochar both as support and adsorbent materials [40]. These results perfectly align with those reported in the literature [20].

Regarding OP sample sizes, an initial investigation was carried out to assess their effect on product distributions from pyrolysis. Fig. 3 (b) proved that as sample size increased, the biochar yield also significantly increased from 27.5 to 35.9 %, while the yields of gas and condensable products decreased. This trend in biochar yield could be attributed to the higher surface area of smaller samples, which during pyrolysis can form volatile products that leave the biomass structure without undergoing secondary cracking reactions [41]. In contrast, larger biomasses are more affected by secondary cracking due to limited heat and mass transfer. The visible structures of the obtained biochars from the SEM analysis are reported in Fig. 3 (c-e) showing a similar morphology. Regarding condensable products, an increase in sample size led to a decrease in their overall yield. The pyrogas yield (35 %) was the highest when OP samples of 1.0 × 1.0 cm^2 were used. In comparison, the smallest (0.5 × 0.5 cm^2) and largest (2.0 × 2.0 cm^2) biomasses resulted in comparatively lower gas release. The pyrogas trend agreed with the study of Abbas et al. which tested different meshes and proved that the intermediate ones released higher amounts of gas [42].

Differences were observed in the chemical and physical properties between the 0.5 × 0.5 cm^2, 1.0 × 1.0 cm^2, and 2.0 × 2.0 cm^2 samples (Table 2). As the sample size increased, the fixed carbon content decreased due to an increase in volatile matter, and the SSA also decreased. These trends are attributed to the limited mass and heat transfer in larger samples. The smallest biochar samples exhibit the highest HHV, which decreases with increasing sample size. This is consistent with the higher carbon content and lower volatile matter in smaller samples, making them more energy-dense. The trends of product distribution and biochar properties agreed with other studies available in the literature on the effect of sample sizes of rice husk, corn cob, and olive residues [43,44] on pyrolysis results. The present study aimed to explore the use of biochar to support microalgae immobilization by proving the technical feasibility of the proposed solution while selecting the one with the lowest environmental impact. To achieve this, an OP sample size of 1.0 × 1.0 cm^2 was chosen as a balance between product distribution (biochar, bio-oil, and pyrogas), effective immobilization, and desirable physico-chemical properties. This ensured suitability for both the immobilization process and its future applications.

3.3. *Bioremediation studies*

The results from scenario 1 are shown in Fig. 4 (a, b), highlighting the phenolic compound removal performance of free microalgae and the two OP substrates, with and without the attached cells. Bioremediation of phenolic compounds by *C. vulgaris* cells was performed at 5 and 10 % *v*/v olive mill wastewater (OMWW) and both graphs show a reduction in

Table 2
Chemical and physical characterization of the obtained biochar samples with different dimensions and comparison with literature studies concerning OP-derived biochar.

Parameter	Biochar samples (cm^2) from this study			Literature data
	0.5 × 0.5	1.0 × 1.0	2.0 × 2.0	
Moisture (%)	3.40 ± 0.09	2.23 ± 0.09	2.01 ± 0.08	3.20–6.20 [45,46]
Ashes (%)	9.89 ± 1.00	7.32 ± 1.08	4.78 ± 0.23	6.90–7.80 [28,45,46]
Volatile matter (%)	32.34 ± 1.20	37.67 ± 1.00	40.23 ± 0.90	21.40–33.40 [28,45,46]
Fixed carbon (%)	54.37 ± 3.89	52.78 ± 2.32	52.98 ± 1.96	55.20–64.80 [28,28,45,46]
C (%)	70.80 ± 1.00	67.70 ± 0.90	66.80 ± 0.20	80.72 [47]
H (%)	4.90 ± 0.20	3.70 ± 0.10	4.5 ± 0.27	4.00 [28]
N (%)	2.20 ± 0.01	2.20 ± 0.01	1.50 ± 0.01	1.20–2.55 [28,46,47]
S (%)	0.10 ± 0.001	0.10 ± 0.001	0.10 ± 0.001	0.00 [28]
O (%)	21.90 ± 0.30	26.40 ± 0.10	27.1 ± 0.02	16.16–31.30 [28,47]
pH	8.76 ± 0.90	8.53 ± 0.20	8.21 ± 0.20	9–9.97 [45,46]
HHV (MJ/kg)	31.24 ± 0.01	28.14 ± 0.08	28.72 ± 0.02	nd
Average SSA (m^2/g)	102.35	96.06	80.98	70.00–352.50 [28,47]
Average pore volume (cm^3/g)	0.043	0.032	0.019	0.018–0.15 [28,47]

HHV, higher heating value; SSA, specific surface area.

phenolic compound content over time across all treatments. The negative control (red bars) consistently shows the least reduction in phenolic compound content, maintaining high levels across all time points. This indicates that natural (photo)degradation is minimal without appropriate treatment. Analysis of wastewater samples taken at predetermined time points shows that phenolic compound removal underwent a first adaptation phase of the microalgae and then improved in the last time points in both conditions. The residual content with free cells was significantly lower than that by immobilized cells and OP alone, only when 5 % *v*/v OMWW was used. The phenolic compound content from 5 % *v*/v OMWW solutions respectively with free and immobilized cells was 75 % and 89 % within 24 h and in 7 days was 29 % and 38 % (* $p < 0.05$). On the other hand, with 10 % *v*/v OMWW, both free and immobilized cells had similar phenolic compound removal percentages (~ 77 %) after 7 days, which was significantly higher than that by empty OP (42 %) (Fig. 4 (b)). This observation suggests that the direct exposure of free microalgae to phenolic compounds facilitates quicker uptake and metabolic processing without the diffusion limitations imposed by the immobilization matrix. However, at higher OMWW concentrations, stress factors such as osmotic pressure and toxicity reduce their activity compared to immobilized cells, which benefit from the protective environment provided by the OP substrate [48]. Several protective benefits could be offered by OP to mitigate the adverse effects of these toxic factors; in particular, the OP can act as a physical barrier, shielding the microalgae from direct exposure to high concentrations of pollutants and allowing the microalgae to adapt more effectively. Moreover, longer time periods are usually needed for phenolic molecules to interact with the microalgae in the immobilization support since the pollutants require time to diffuse into the matrix and interact with the cells [49,50].

COD values are often used as indicators of water quality as they measure the amount of organic compounds present in wastewater. The percentage of residual COD from OMWW is shown in Fig. 4 (c, d). Free microalgae treatment (blue bars) significantly reduces COD levels, but not as effectively as the OP with immobilized microalgae (OPM) treatment. On the completion of the biodegradation experiment (~ 168 h), the COD levels of the wastewater were reduced by 77 and 59 % for 5 *v*/v and 10 % *v*/v OMWW, respectively in the case of microalgae immobilized on OP. In the case of COD removal, these could be considered quite high values, taking into account the dark color of the OMWW, which hinders the cells' performance. No significant differences were noted between free microalgae and immobilized microalgae in both experimental conditions.

Overall, the OPM treatment consistently outperforms both free microalgae and orange peel alone, especially over extended treatment times. This suggests that the immobilization of microalgae on orange peel enhances their ability to degrade organic pollutants, possibly due to improved stability and interaction with the wastewater.

The results from scenario 2 with the OP-derived biochar are shown in Fig. 5. Here the biochar-microalgae complex was more effective in removing phenolic compounds than the free microalgae and empty biochar and it was significantly noted after 72 and 168 h for both conditions. In particular, the residual phenolic compound content was 44 % and 31 % for 5 % and 10 % *v*/v OMWW, respectively, from solutions with microalgae immobilized on biochar samples. The statistically significant smaller uptake of phenolic compounds when using free cells with 10 % *v*/v OMWW may be attributed to their aggregation (Fig. 6 (b)) due to electrostatic interaction between them, thus reducing their three-dimensional surface area for adsorption, as already reported in the literature [51]. It can be hypothesized that the pore structure of biochar (Fig. 3 (d)) provides an internal living environment for microalgae and protects them from external pollutants, allowing them to increase their survival in a contaminated environment, as already suggested by other authors working with microorganisms [52]. Microalgae immobilized within biochar pores likely shifted from strictly photosynthetic to mixotrophic and, in some cases, heterotrophic modes of metabolism, particularly for cells living in deeper or smaller pores. In fact, in environments with low light availability or high concentrations of organic substrates (such as the present one), the microalgae frequently adopted a heterotrophic strategy, relying entirely on organic carbon. This metabolic flexibility, common in species like *Chlorella*, allows immobilized microalgae to sustain growth under suboptimal light conditions [53]. Additionally, biochar's intrinsic adsorption properties concentrated phenolic compounds and other organic contaminants near the microalgae, increasing their bioavailability for degradation. This proximity likely enhanced the microalgae's metabolic activity on these complex pollutants, as reflected in the improved removal rates observed.

The percentage residual COD from OMWWW is shown in Fig. 5 (c, d). A similar trend is observed among COD and phenolic compound removal results. For 5 % *v*/v OMWW, a residual COD of 45 and 29 % for free and immobilized microalgae, respectively, is reported, while it is reported to be 57 and 41 % in the case of OMWW 10 % *v*/v. Higher values were expected when performing experiments with an initial higher load of COD content.

The results for COD reduction using immobilized microalgae in this study indicate that approximately 60 % of the COD was removed using both the OPM (Fig. 4 (d)) and BM (Fig. 5 (d)) systems. It must be underlined that the novelty of this work lies in the fact that it is the first study to combine both biochar or OP as substrates with microalgae for OMWW bioremediation. This dual approach, integrating both physical support and biological treatment, presents a unique strategy that makes direct comparisons with existing literature challenging, as similar methods have not been previously investigated. As one of the closest examples, the study of Bleve et al. [54] reported the treatment of OMWW with the yeast strain *Geotrichum candidum* which was selected for whole-cell immobilization in calcium alginate gel. The COD reduction was ~30 % after 7 days. Similarly, Neifar et al. [55] studied the OMWW bioremediation activity of white-rot fungi *Pycnoporus coccineus* and *Coriolopsis polyzona* immobilized on polyurethane foam. The study reported a COD removal of 30–40 % for both strains after 7 days of

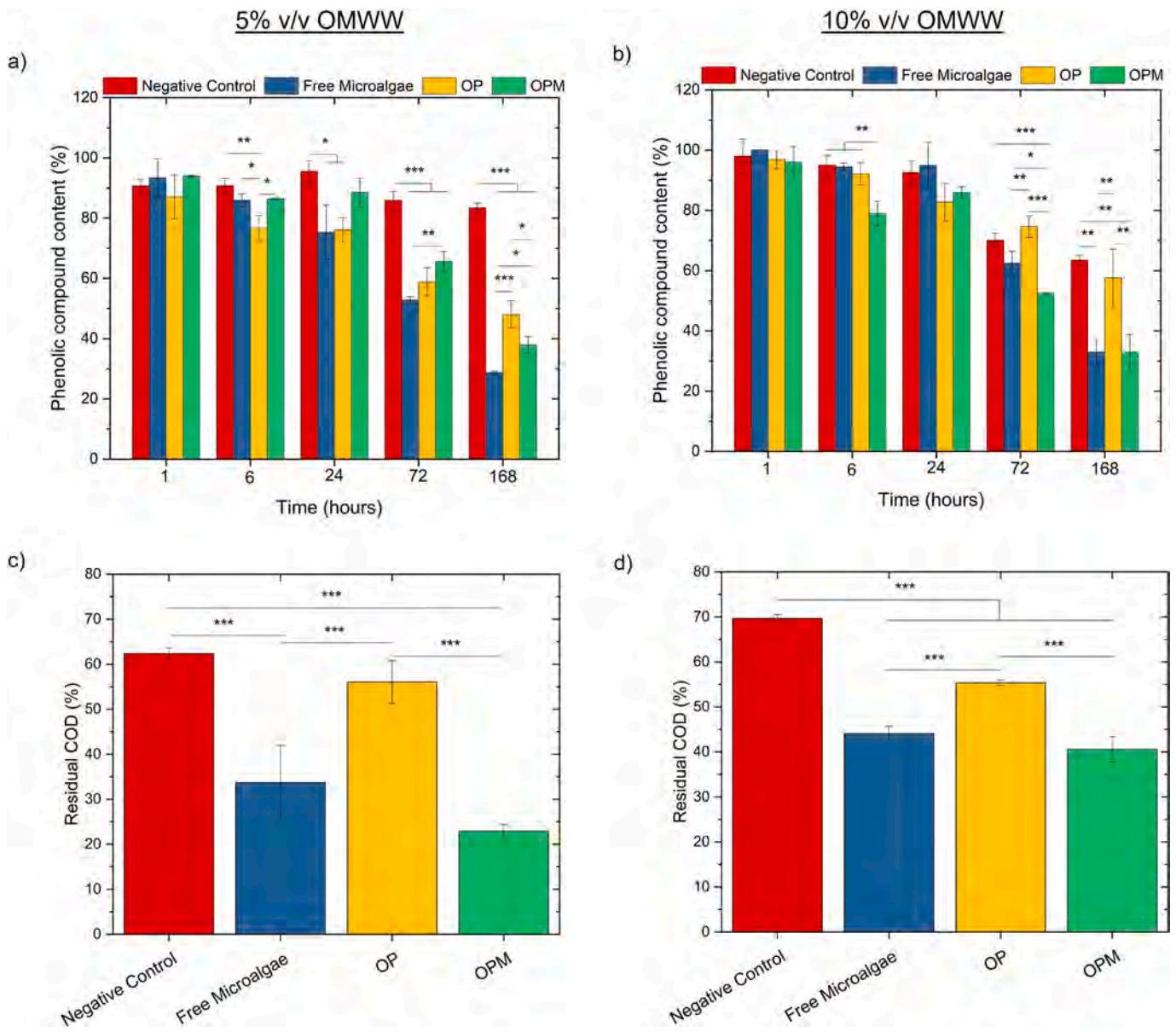

Fig. 4. Bioremediation results from scenario 1. Percentages of phenolic compound content (a, b) and residual COD (c, d) in the OMWW samples under light (red) or during the treatment with free microalgae (blue), orange peel (yellow), or immobilized microalgae (green) at different time points. * $p < 0.05$, ** $p < 0.01$, *** $p < 0.001$.

treatment. However, it should be noted that the efficiency of COD removal can be influenced by several variables, such as eventual pre-treatment of OMWW, starting cell and COD concentration, and light intensity.

Overall, results evidence that the treatment with biochar with immobilized microalgae (BM) was the most effective method for reducing both phenolic compounds content and COD in OMWW. BM consistently outperforms both biochar and free microalgae treatments, particularly at later stages of the treatment process (72 and 168 h). Together, these findings demonstrate that biochar not only serves as a physical support but also actively contributes to creating an optimized microenvironment, amplifying the microalgae's pollutant removal capacity. The combination of adsorption, protective microenvironments, and metabolic flexibility in immobilized microalgae within biochar highlights the synergy between physical and biological processes. These mechanisms collectively amplify the pollutant removal efficiency and offer insights for scaling up bioremediation strategies. This synergy suggests that biochar-immobilized microalgae could serve as an effective, sustainable strategy for treating complex agricultural effluents like olive mill wastewater, with implications for broader wastewater applications.

3.4. *Characterization of the products from bioremediation studies*

At the end of the bioremediation experiments, the substrates - either OP or biochar - with immobilized microalgae (OPM and BM) can be described as "exhausted" substrates. These were characterized after the treatment process and results are reported in Fig. 6. The fibrous network of the orange peel was homogeneously covered by immobilized *C. vulgaris* cells, as seen in Fig. 6 (a), with the relative SEM image showing these cells well-integrated onto the fibrous threads even after 7 days (Fig. 6 (c)). The *C. vulgaris* cells were observed to strongly adhere and form a biofilm-like structure onto the surface of the substrates as well as inside the pores. This type of immobilization could initially occur as a result of natural adsorption followed by active growth within the microalgae biofilm. The FTIR spectrum (Fig. 6 (e)) of *C. vulgaris* exhibits

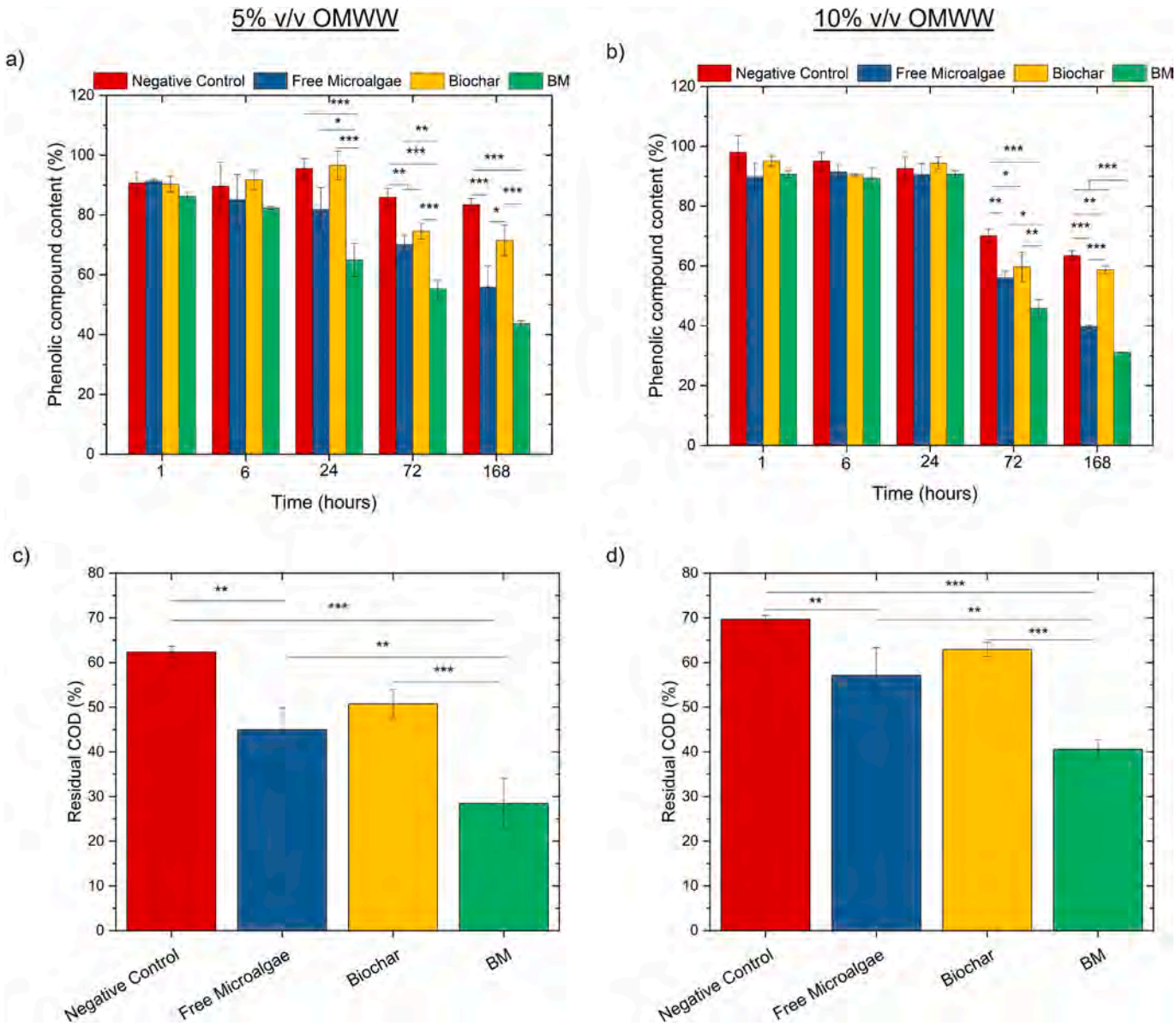

Fig. 5. Bioremediation results from scenario 2. Percentages of phenolic compound content (a, b) and residual COD (c, d) in the OMWW samples under light (red) or during the treatment with free microalgae (blue), biochar (yellow) or immobilized microalgae (green) at different time points. * $p < 0.05$, ** $p < 0.01$, *** $p < 0.001$.

several characteristic absorption bands corresponding to the functional groups present in its biochemical composition (full assignment of the bands is reported in Table S6). The broad peak at 3277 cm^{-1} is indicative of O—H stretching vibrations. Peaks at 2961, 2927, and 2872 cm^{-1} are attributed to C—H stretching vibrations, mainly reflecting the presence of aliphatic chains in lipids and proteins. The band at 1733 cm^{-1} corresponds to C═O stretching vibrations, likely from ester carbonyls in lipids. A prominent peak at 1644 cm^{-1} can be associated with the amide I band, while the absorption at 1539 cm^{-1} is assigned to the amide II band, further indicating protein content. The peaks at 1456 and 1395 cm^{-1} are linked to C—H bending vibrations, while the band at 1339 cm^{-1} could be associated with C—N stretching in amines. The peak at 1238 cm^{-1} is characteristic of P═O stretching in phospholipids and phosphate groups, while the prominent peak at 1030 cm^{-1} is indicative of C-O-C stretching in polysaccharides. The smaller peaks at 923 and 864 cm^{-1} may represent out-of-plane bending vibrations of aromatic rings [56,57].

The FTIR spectrum of the sample with microalgae immobilized on OP at the end of the experiments exhibits similar peaks to the spectrum of *C. vulgaris,* even if several overlapped peaks from the OP structure can be observed. The slightly shifted bands indicate the involvement of hydroxyl and carbonyl groups in the immobilization of microalgae to the OP surface (Table 3). A significant reduction in the intensity of some of the bands (e.g., the one detected at 1644 cm^{-1}) is also visible in the spectrum of immobilized microalgae. Functional groups (e.g., C-O-C stretching) in polysaccharides also contribute to the adsorption process through van der Waals forces and hydrogen bonding, while aromatic rings could engage in π-π interactions with phenolic compounds [58]. The presence of functional groups on the cell wall, such as those from phospholipids, can be the leading contribution towards the biosorption process of polyphenols. In particular, as suggested by previous literature, polyphenols have the ability to form hydrogen bonds between their hydroxyl group and the C═O and phosphate groups of lipids [59]. This could cause the shift of the observed peaks (e.g., at 552 cm^{-1}) towards lower frequencies.

On the other hand, the immobilization of microalgae on the surface of biochar seems less homogeneous (Fig. 6 (b)), probably because most of the biochar support was floating on the top of the water surface.

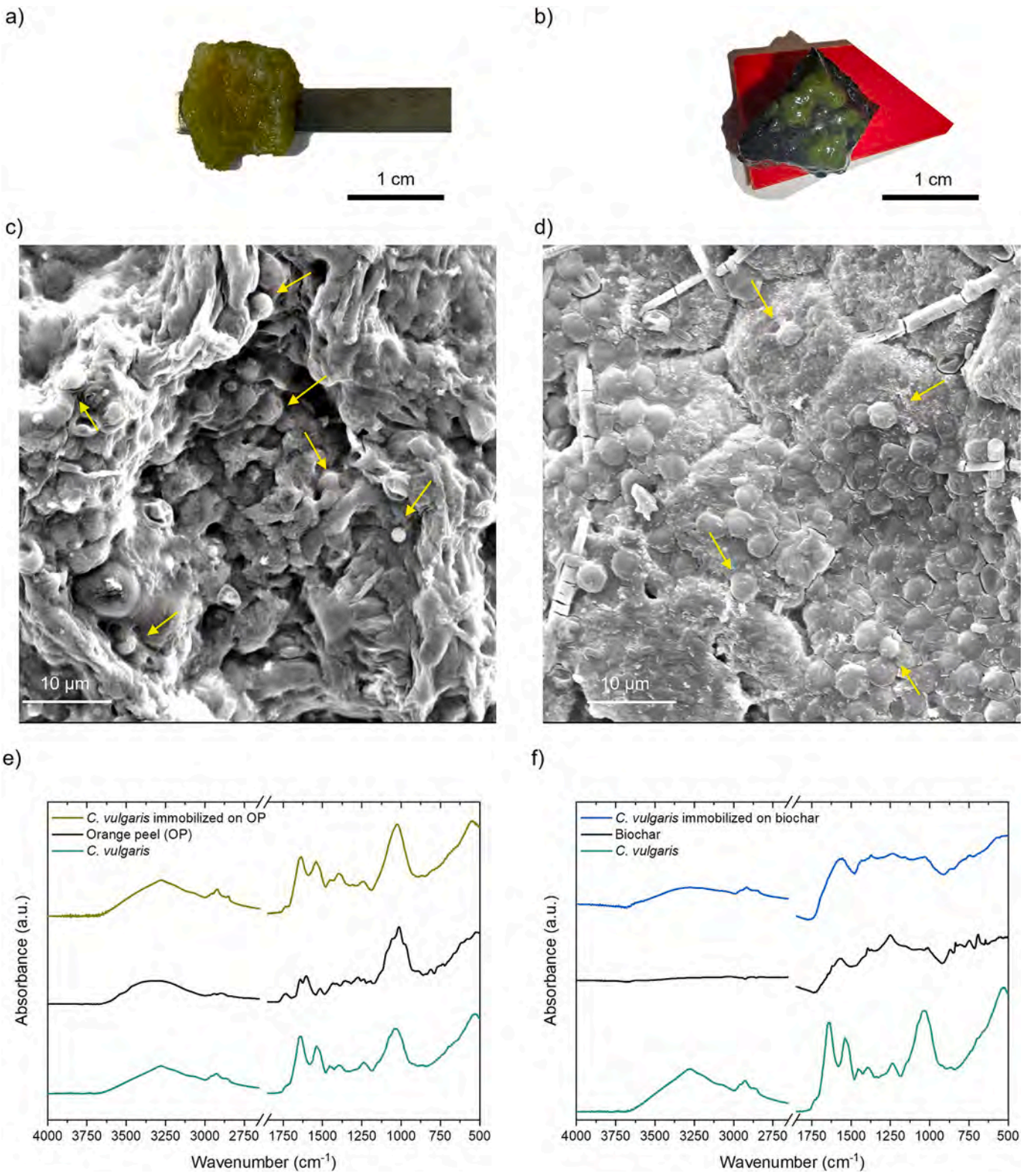

Fig. 6. Characterization of the final microalgae-matrix supports at the end of the experiments. Digital photos (a, b) and SEM images (c, d) of the microalgae-immobilized complex for OP and OP-derived biochar, respectively. Yellow arrows indicate the presence of microalgae cells (with an average diameter of 4 μm). FTIR spectra show the graphs from single components (microalgae *C. vulgaris*, fresh orange peel, and empty biochar) and from the microalgae-immobilized substrates.

Microalgae are observed to grow in large clusters within their biofilm, as also confirmed by the SEM image (Fig. 6 (d)). In the FTIR spectrum of empty biochar (full assignment of the bands is reported in Table S7), the peak at 1568 cm^{-1} is associated with C═C stretching vibrations, indicative of aromatic rings and unsaturated carbon structures, which are typical features of biochar due to the pyrolysis process. Peaks at 1394 cm^{-1} and 1372 cm^{-1} correspond to C—H bending vibrations in aliphatic and aromatic hydrocarbons. The band at 1251 cm^{-1} can be

Table 3
Shifted FTIR peaks and their assignments for immobilized microalgae on orange peel (OPM) and biochar (BM), along with their implications for the bioremediation mechanism.

Shifted peak (cm^{-1}) in the FTIR spectrum of immobilized microalgae		Assignment	Implication for bioremediation mechanism(s)
on OP (OPM)	on biochar (BM)		
3280	3278	O-H stretching vibrations	Involvement of hydroxyl groups in biosorption process by facilitating hydrogen bonding and electrostatic interactions
2956, 2921, 2851	2961, 2927, 2872	C-H stretching vibrations (lipids, proteins)	The presence of aliphatic chains from lipids and proteins, potentially involved in polyphenol interactions, contributes to the adsorption of phenolic compounds through hydrophobic interactions and van der Waals forces.
1651		C=O (amide I) and C=C stretching	Involvement of carbonyl groups from proteins and lipid groups in the interaction with polyphenols
	1540	N-H bending (amide II)	Involvement of amino groups from proteins in the interaction with polyphenols through hydrogen bonding and electrostatic interactions
1447, 1397	1389	C-H bending	Presence of lipids/proteins involved in biosorption.
1240	1237	P=O stretching	Phospholipids and phosphate groups on microalgae cell wall involved in polyphenol biosorption by forming hydrogen bonds
1022	1159, 1032	C-O-C and C-O-H stretching	Polysaccharides and oxygenated groups in both biochar and microalgae contribute to polyphenol interactions by facilitating hydrogen bonding and electrostatic interactions
902, 809, 745, 520		C-H and O—H bending	Aromatic groups could link with polyphenols via π-π interactions during biosorption.

attributed to C—O stretching vibrations, highlighting the presence of oxygenated functional groups in the biochar. The intensity at 1162, 1065, 1041, and 1024 cm^{-1} (C-O-C and C—O vibrations in cellulose and hemicellulose) decreased with respect to OP spectrum, due to polysaccharide degradation processes [60]. The peaks between 870 and 540 cm^{-1} are characteristic of out-of-plane bending vibrations of aromatic C—H, reflecting the presence of polycyclic aromatic hydrocarbons [61]. In the opposite manner with respect to scenario 1, the FTIR spectrum of microalgae immobilized on biochar at the end of the experiments exhibits a similar shape and peaks' positions to the spectrum of empty biochar, even if several peaks assigned to microalgae groups can be observed (e.g., at 3278 and around 2900 cm^{-1}). After *C. vulgaris* cells were attached to the biochar, the increase in peaks at 1555, 1389, and 1032 cm^{-1} was observed, which could originate from the component of the microalgae surfaces. These functional groups facilitate the adsorption of phenolic compounds through hydrogen bonding, electrostatic interactions, and π-π interactions, contributing to the overall bioremediation process (Table 3).

3.5. Environmental analysis

The environmental analysis compared scenario 1 and scenario 2, considering the microalgae-based bioremediation of OMWW at 5 and 10 % *v*/v through OP and OP-derived biochar. The ex-ante Life Cycle Assessment (LCA) evaluated the impact on the functional unit (FU) equal to 10 g of OP. The environmental scores (reported in Table 4) were calculated with ReCiPe 2016 MidPoint (H), which includes 18 impact categories. Aligned with the European Green Deal's target of achieving net-zero emissions by 2050, the ex-ante LCA focused on climate change impact, with other environmental impacts considered as follow-up indicators.

Table 4
Environmental impacts calculated with ReCiPe 2016 MidPoint (H) and referring to the FU = 10 g of OP. The elaboration was performed with the database Ecoinvent 3.8.5.

Impact category	Unit	OMWW			
		Scenario 1		Scenario 2	
		10 % *v*/v	5 % *v*/v	10 % *v*/v	5 % *v*/v
Global warming	kg CO_2 eq	0.426	0.947	0.518	0.522
Stratospheric ozone depletion	kg CFC11 eq	0.385 × 10^{-6}	0.639 × 10^{-6}	0.430 × 10^{-6}	0.430 × 10^{-6}
Ionizing radiation	kBq Co-60 eq	75.8 × 10^{-3}	113 × 10^{-3}	82.310^{-3}	82.410^{-3}
Ozone formation. Human health	kg NOx eq	0.900 × 10^{-3}	1.54 × 10^{-3}	1.02 × 10^{-3}	1.02 × 10^{-3}
Fine particulate matter formation	kg PM2.5 eq	0.594 × 10^{-3}	0.966 × 10^{-3}	0.662 × 10^{-3}	0.666 × 10^{-3}
Ozone formation. Terrestrial ecosystems	kg NOx eq	0.912 × 10^{-3}	1.57 × 10^{-3}	1.03 × 10^{-3}	1.04 × 10^{-3}
Terrestrial acidification	kg SO_2 eq	1.81 × 10^{-3}	2.88 × 10^{-3}	2.00 × 10^{-3}	2.01 × 10^{-3}
Freshwater eutrophication	kg P eq	137 × 10^{-6}	218 × 10^{-6}	153 × 10^{-6}	155 × 10^{-6}
Marine eutrophication	kg N eq	20.2 × 10^{-6}	25.7 × 10^{-6}	21.2 × 10^{-6}	21.3 × 10^{-6}
Terrestrial ecotoxicity	kg 1.4-DCB	534 × 10^{-3}	937 × 10^{-3}	609 × 10^{-3}	617 × 10^{-3}
Freshwater ecotoxicity	kg 1.4-DCB	10.8 × 10^{-3}	18.8 × 10^{-3}	12.2 × 10^{-3}	12.3 × 10^{-3}
Marine ecotoxicity	kg 1.4-DCB	14.0 × 10^{-3}	24.6 × 10^{-3}	15.9 × 10^{-3}	16.0 × 10^{-3}
Human carcinogenic toxicity	kg 1.4-DCB	13.9 × 10^{-3}	24.6 × 10^{-3}	15.8 × 10^{-3}	16.0 × 10^{-3}
Human non-carcinogenic toxicity	kg 1.4-DCB	246 × 10^{-3}	399 × 10^{-3}	274 × 10^{-3}	276 × 10^{-3}
Land use	m2a crop eq	19.3 × 10^{-3}	26.9 × 10^{-3}	20.6 × 10^{-3}	20.7 × 10^{-3}
Mineral resource scarcity	kg Cu eq	0.438 × 10^{-3}	0.832 × 10^{-3}	0.510 × 10^{-3}	0.516 × 10^{-3}
Fossil resource scarcity	kg oil eq	116 × 10^{-3}	292 × 10^{-3}	148 × 10^{-3}	150 × 10^{-3}
Water consumption	m^3	10.8 × 10^{-3}	16.1 × 10^{-3}	11.8 × 10^{-3}	11.8 × 10^{-3}

The bioremediation performed with immobilized microalgae on OP in OMWW at 10 % *v*/v (scenario 1) reached the lowest impact (0.426 $kgCO_2$ eq/FU), followed by the bioremediation conducted with OP-derived biochar in OMWW at 10 and 5 % *v*/v (scenario 2) with 0.518 and 0.522 $kgCO_2$ eq/FU, respectively. Lastly, the immobilized microalgae on OP treating OMWW at 5 % *v*/v (scenario 1) showed the highest impact (0.947 $kgCO_2$ eq/FU). Significant differences were observed in scenario 1 with OMWW at 10 % and 5 % *v*/v, as the 10 % *v*/v resulted in higher bioremediation yields, greater energy content in pyrogas, and lower energy consumption due to the reduced water content from the lower dilution. In contrast, scenario 2 with OMWW at 10 % and 5 % *v*/v showed no significant differences, as the bioremediation and pyrolysis yield at 10 % *v*/v were only slightly higher than those at 5 % *v*/v.

The importance of energy recovery from slow pyrolysis was evaluated through the sensitivity analysis in which bio-oil was considered an energy carrier and not a waste (see Table 5). The sensitivity analysis

Table 5
Impacts calculated with ReCiPe 2016 MidPoint (H) based on the sensitivity analysis where bio-oil is considered an energy carrier.

Impact category	Unit	OMWW			
		Scenario 1		Scenario 2	
		10 % *v*/v	5 % *v*/v	10 % *v*/v	5 % *v*/v
Global warming	kg CO_2 eq	−1.02	0.110	−0.498	−0.494
Stratospheric ozone depletion	kg CFC11 eq	−0.290 × 10^{-6}	0.247 × 10^{-6}	0.0353 × 10^{-6}	0.035 × 10^{-6}
Ionizing radiation	kBq Co-60 eq	−18.2 × 10^{-3}	58.6 × 10^{-3}	43.0 × 10^{-3}	43.1 × 10^{-3}
Ozone formation. Human health	kg NOx eq	−0.784 × 10^{-3}	0.566 × 10^{-3}	0.0552 × 10^{-3}	0.0628 × 10^{-3}
Fine particulate matter formation	kg PM2.5 eq	−0.361 × 10^{-3}	0.411 × 10^{-3}	0.160 × 10^{-3}	0.164 × 10^{-3}
Ozone formation. Terrestrial ecosystems	kg NOx eq	−0.818 × 10^{-3}	0.569 × 10^{-3}	0.0375 × 10^{-3}	0.0458 × 10^{-3}
Terrestrial acidification	kg SO_2 eq	−0.926 × 10^{-3}	1.29 × 10^{-3}	0.614 × 10^{-3}	0.624 × 10^{-3}
Freshwater eutrophication	kg P eq	−62.7 × 10^{-6}	102 × 10^{-6}	58.5 × 10^{-6}	60.5 × 10^{-6}
Marine eutrophication	kg N eq	6.22 × 10^{-6}	17.6 × 10^{-6}	14.6 × 10^{-6}	14.7 × 10^{-6}
Terrestrial ecotoxicity	kg 1.4-DCB	-503 × 10^{-3}	335 × 10^{-3}	38.9 × 10^{-3}	46.9 × 10^{-3}
Freshwater ecotoxicity	kg 1.4-DCB	−9.75 × 10^{-3}	6.83 × 10^{-3}	1.42 × 10^{-3}	1.52 × 10^{-3}
Marine ecotoxicity	kg 1.4-DCB	−13.6 × 10^{-3}	8.61 × 10^{-3}	0.970 × 10^{-3}	1.09 × 10^{-3}
Human carcinogenic toxicity	kg 1.4-DCB	−14.4 × 10^{-3}	8.24 × 10^{-3}	−0.665 × 10^{-3}	−0.534 × 10^{-3}
Human non-carcinogenic toxicity	kg 1.4-DCB	-144 × 10^{-3}	172 × 10^{-3}	77.9 × 10^{-3}	79.9 × 10^{-3}
Land use	m2a crop eq	−0.192 × 10^{-3}	15.6 × 10^{-3}	11.0 × 10^{-3}	11.0 × 10^{-3}
Mineral resource scarcity	kg Cu eq	−0.609 × 10^{-3}	0.225 × 10^{-3}	−0.137 × 10^{-3}	−0.131 × 10^{-3}
Fossil resource scarcity	kg oil eq	-375 × 10^{-3}	8.05 × 10^{-3}	−212 × 10^{-3}	-210 × 10^{-3}
Water consumption	m^3	-2.30 × 10^{-3}	8.49 × 10^{-3}	6.32 × 10^{-3}	6.38 × 10^{-3}

confirmed the results obtained from the ex-ante LCA, with environmental impacts decreasing across all categories for all scenarios. This reduction is primarily attributed to the energy contributions from pyro-gas and bio-oil, which offset the energy costs associated with immobilization, bioremediation, and pyrolysis. Fig. 7 illustrates the effect of polyphenol recovery and the inclusion of energy carriers (pyro-gas and bio-oil) in the energy balance within the climate change impact category. When both pyro-gas and bio-oil are considered, the impacts decrease by approximately 50–66 %. Fig. 7 also highlights that, across the four tested configurations, the bioremediation process had the highest environmental impact due to its energy requirements and the duration of the tests (168 h).

Scenario 1, with immobilized microalgae on OP in OMWW at 10 % *v*/v, yielded the best results in the sensitivity analysis, achieving the highest polyphenol recovery as well as the highest HHV for both pyrogas and bio-oil. This is likely due to the bioremediation process, which enriched the organic matter matrix, consequently enhancing the quality of the gas and bio-oil.

The contribution of bio-oil warrants further discussion. As a renewable resource, bio-oil has the potential to replace fossil fuels and reduce greenhouse gas emissions. Its versatility is notable, as it can be utilized as both a thermal and electrical energy vector or as a feedstock for advanced fuels. These benefits were considered in the sensitivity analysis, as bio-oil separation from water is feasible at the laboratory scale. As shown in the inventory tables (S1-S5), separating bio-oil from water at this scale required an additional 5 % of electrical energy compared to scenarios where it was not utilized.

However, the industrial-scale use of bio-oil presents challenges that this preliminary study cannot fully address. Key limitations include the chemical composition of bio-oil, which varies based on the type of biomass and the pyrolysis conditions. This variability complicates the establishment of industrial standards and the development of a standardized refining process [62]. Additionally, bio-oil has a lower calorific value compared to fossil fuels, and its high oxygen content can cause corrosion issues in processing equipment. Long-term storage and transportation of bio-oil are also challenging due to its instability, tendency to degrade, and the need for specific preservation conditions [63]. From an economic perspective, bio-oil plants for bio-oil production and utilization require significant investment costs and may not be economically competitive without subsidies [62]. Given these considerations, this study has adopted a cautious approach, treating bio-oil as a waste product, while the sensitivity analysis evaluates its potential for utilization.

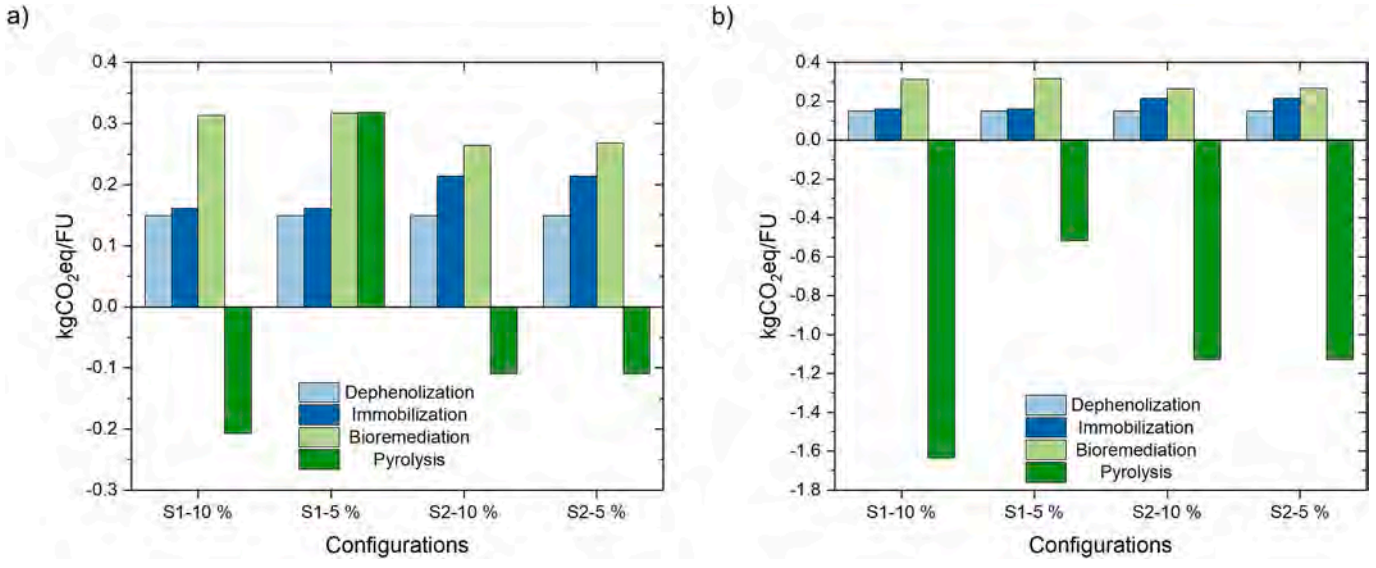

Fig. 7. Global warming as climate change impact category considering a) bio-oil as waste and b) bio-oil as an energy carrier for scenarios 1 (S1) and 2 (S2).

Upon analyzing the data in Table 4, scenario 1 with OMWW at 10 % *v*/v exhibited the lowest environmental impacts. The categories in which it significantly differs from the other scenarios are water consumption, freshwater eutrophication, terrestrial acidification, and fossil resource scarcity. In these categories, scenario 1 at 10 % *v*/v demonstrates its strengths. Specifically, the lower dilution of OMWW compared to the 5 % *v*/v scenario reduced water consumption, while the higher polyphenol degradation contributed to lower impacts in freshwater eutrophication and terrestrial acidification. Additionally, the higher energy recovery during pyrolysis mitigated the increase in fossil resource consumption relative to the other scenarios. These findings offer an alternative to the current practice of treating OMWW by diluting it with fresh water or water from other waste streams [64].

Furthermore, the study of Manthos et al. [64] considered the direct application of OMWW to land and freshwater eutrophication, and terrestrial acidification are around 20 % higher than the ones achieved in the present study (calculated by moving from the FU of the study of Manthos et al. [64] to the one of the present study).

It must be noted that, to date, there are no available studies concerning the environmental impacts associated with microalgae immobilization on supports. There are studies investigating the environmental impacts of the cultivation of microalgae, conversion of microalgae to pharmaceutical and biodiesel products, and biochar production. Regarding the environmental impacts of biochar production, most of the literature studies underline the importance of obtaining product yields and products with energy content sufficient to cover the energy costs of pyrolysis.

Some reviews investigated the potentiality of biochar for water treatment to achieve Sustainable Development Goal 6 (Ensure availability and sustainable management of water and sanitation for all by 2030). Gwenzi et al. [65] defined biochar as a low-cost renewable alternative to classic systems like sand filtration, boiling, solar disinfection, and chlorination.

Additionally, while current methods primarily focus on pathogen removal, biochars have demonstrated the ability to remove chemical (e.g., methylene blue, metals, organic compounds), biological, and physical contaminants [66]. Studies have also shown that biochar, after being used for water remediation, can be applied to soil to enhance soil quality and improve crop yields by releasing adsorbed nutrients [65]. A major challenge for biochar's application in water remediation remains the lack of comprehensive environmental assessments and the potential health risks associated with its use [67].

4. Conclusions

This study demonstrates the effectiveness of using microalgae immobilized on orange peel (OP) and OP-derived biochar as innovative, green substrates for the bioremediation of olive mill wastewater (OMWW). Both OMWW and OP are two high-produced byproducts in the Mediterranean area that necessitate a more effective management in the waste system. Both technical and environmental aspects were evaluated. The bioremediation of OMWW at 5 and 10 % *v*/v was explored through *Chlorella vulgaris* immobilized on OP (scenario 1) and OP-derived biochar (scenario 2). The synergistic integration of these waste-derived materials with *C. vulgaris* not only achieved significant removal of environmentally pollutant phenolic compounds and abatement of chemical oxygen demand (COD) but also facilitated sustainable energy recovery through the pyrolysis of spent substrates. Scenario 1 with OMWW at 10 % *v*/v reached the highest performance, achieving ~70 % phenolic compound degradation, ~ 60 % COD abatement, and a climate change impact of 0.43 kg CO_2 per 10 g of fresh OP, and when bio-oil is used as energy carrier the impact decreased to −1.02 kg CO_2 per 10 g of fresh OP. These findings highlight the potential for scaling up the technology to pilot scales. Key challenges include optimizing the adsorbent-to-wastewater ratio, ensuring uniform distribution of microalgae on substrates, maintaining process stability over extended operational periods and addressing variable wastewater compositions. Economic considerations, such as cost-effective sourcing of OMWW, OP, and biochar at the same pilot plant, energy requirements for pyrolysis, and market viability of byproducts (e.g., bio-oil), must also be addressed.

Moreover, this study highlights the significance of considering each stage of the bioremediation process, seeking operational conditions that ensure, firstly, maximal recovery of the high-value product and subsequently the management of process residues through energetic valorization to at least cover the energy costs of the entire process. The results demonstrate the effectiveness of implementing systems aligned with the Waste Framework Directive (prioritizing material recovery over energy recovery) within a bioeconomy perspective. Overall, this study promotes, based on technical feasibility and environmental sustainability, the integrated management of byproducts to obtain valuable products applicable in the agro-industrial sector and pave the way for the development of scalable, resource-efficient waste management solutions that contribute to environmental sustainability and energy self-sufficiency.

Acknowledgment & Funding sources

This study was carried out within the Agritech National Research Center and received funding from the European Union Next-Generation EU (Piano Nazionale di Ripresa e Resilienza (PNRR) – missione 4 componente 2, investimento 1.4 – D.D. 1032 17/06/2022, CN00000022). J. F. B. thanks to Network 4 Energy Sustainable Transition (NEST) - PNRR. This manuscript reflects only the authors' views and opinions, neither the European Union nor the European Commission can be considered responsible for them.

CRediT authorship contribution statement

Martina Lenzuni: Writing – original draft, Visualization, Validation, Methodology, Investigation, Formal analysis, Conceptualization. **Francesca Demichelis:** Writing – original draft, Validation, Methodology, Investigation, Formal analysis, Conceptualization, Data curation, Visualization. **Juan Felipe Basbus:** Writing – review & editing, Investigation. **Antonio Barbucci:** Writing – review & editing, Investigation. **Francesco Savorani:** Writing – review & editing, Resources, Project administration, Funding acquisition, Conceptualization. **Tonia Tommasi:** Writing – review & editing, Supervision, Resources, Project administration, Funding acquisition, Conceptualization. **Alessandro Alberto Casazza:** Writing – review & editing, Supervision, Resources, Project administration, Methodology, Funding acquisition, Conceptualization.

Declaration of competing interest

The authors declare that they have no known competing financial interests or personal relationships that could have appeared to influence the work reported in this paper.

Data availability

Data will be made available on request.

Appendix A. Supplementary data

Supplementary data to this article can be found online at https://doi.org/10.1016/j.susmat.2025.e01338.

References

[1] M.R. Panuccio, F. Marra, A. Maffia, C. Mallamaci, A. Muscolo, Recycling of agricultural (orange and olive) bio-wastes into ecofriendly fertilizers for improving

soil and garlic quality, Res. Conservat. Recycl. Adv. 15 (2022) 200083, https://doi.org/10.1016/j.rcradv.2022.200083.
[2] M. Lenzuni, A. Converti, A.A. Casazza, From laboratory- to industrial-scale plants: future of anaerobic digestion of olive mill solid wastes, Bioresour. Technol. 394 (2024) 130317, https://doi.org/10.1016/j.biortech.2024.130317.
[3] M. Lenzuni, G. D'Agostino, P. Perego, A. Converti, A.A. Casazza, Insights into the effects of phenolic compounds on the growth of Chlorella vulgaris: the case of olive mill wastewater, Sci. Total Environ. 958 (2025) 177944, https://doi.org/10.1016/j.scitotenv.2024.177944.
[4] E. Tsagaraki, H.N. Lazarides, K.B. Petrotos, Olive Mill Wastewater Treatment, Springer, 2007, pp. 133–157.
[5] E. Spennati, A.A. Casazza, A. Converti, M.P. Padula, F. Dehghani, P. Perego, P. Valtchev, Winery waste valorisation as microalgae culture medium: a step forward for food circular economy, Sep. Purif. Technol. 293 (2022) 121088, https://doi.org/10.1016/j.seppur.2022.121088.
[6] L.E. De Bashan, Y. Bashan, Immobilized microalgae for removing pollutants: review of practical aspects, Bioresour. Technol. 101 (2010) 1611–1627, https://doi.org/10.1016/j.biortech.2009.09.043.
[7] M. Han, C. Zhang, S.-H. Ho, Immobilized microalgal system: an achievable idea for upgrading current microalgal wastewater treatment, Environ. Sci. Ecotechnol. 14 (2023) 100227, https://doi.org/10.1016/j.ese.2022.100227.
[8] N. Akhtar, A. Saeed, M. Iqbal, Chlorella sorokiniana immobilized on the biomatrix of vegetable sponge of Luffa cylindrica: a new system to remove cadmium from contaminated aqueous medium, Bioresour. Technol. 88 (2003) 163–165, https://doi.org/10.1016/S0960-8524(02)00289-4.
[9] K. Athira, A. Sathish, K. Nithya, A. Guhananthan, Corn cob immobilised Chlorella sorokiniana for the sequestration of chromium ions from aqueous solution, Mater. Today: Proceed. 33 (2020) 2148–2155, https://doi.org/10.1016/j.matpr.2020.03.151.
[10] T. Garbowski, M. Pietryka, K. Pulikowski, D. Richter, The use of a natural substrate for immobilization of microalgae cultivated in wastewater, Sci. Rep. 10 (2020) 7915, https://doi.org/10.1038/s41598-020-64656-3.
[11] R. Li, B. Wang, A. Niu, N. Cheng, M. Chen, X. Zhang, Z. Yu, S. Wang, Application of biochar immobilized microorganisms for pollutants removal from wastewater: a review, Sci. Total Environ. 837 (2022) 155563, https://doi.org/10.1016/j.scitotenv.2022.155563.
[12] Y. Shen, H. Li, W. Zhu, S.-H. Ho, W. Yuan, J. Chen, Y. Xie, Microalgal-biochar immobilized complex: a novel efficient biosorbent for cadmium removal from aqueous solution, Bioresour. Technol. 244 (2017) 1031–1038, https://doi.org/10.1016/j.biortech.2017.08.085.
[13] G. Pallas, M.G. Vijver, W.J.G.M. Peijnenburg, J. Guinée, Life cycle assessment of emerging technologies at the lab scale: the case of nanowire-based solar cells, J. Ind. Ecol. 24 (2020) 193–204, https://doi.org/10.1111/jiec.12855.
[14] B.A. Wender, R.W. Foley, V. Prado-Lopez, D. Ravikumar, D.A. Eisenberg, T. A. Hottle, J. Sadowski, W.P. Flanagan, A. Fisher, L. Laurin, M.E. Bates, I. Linkov, T. P. Seager, M.P. Fraser, D.H. Guston, Illustrating anticipatory life cycle assessment for emerging photovoltaic technologies, Environ. Sci. Technol. 48 (2014) 10531–10538, https://doi.org/10.1021/es5016923.
[15] M. Rehan, N.A.M. Abdel-Wahed, A. Farouk, M.M. El-Zawahry, Extraction of valuable compounds from orange peel waste for advanced functionalization of cellulosic surfaces, ACS Sustain. Chem. Eng. 6 (2018) 5911–5928, https://doi.org/10.1021/acssuschemeng.7b04302.
[16] M.G. Shehata, T.S. Awad, D. Asker, S.A. El Sohaimy, N.M. Abd El-Aziz, M. M. Youssef, Antioxidant and antimicrobial activities and UPLC-ESI-MS/MS polyphenolic profile of sweet orange peel extracts, current research in food, Science 4 (2021) 326–335, https://doi.org/10.1016/j.crfs.2021.05.001.
[17] P.F. Ferrari, M. Pettinato, A.A. Casazza, G. De Negri Atanasio, D. Palombo, P. Perego, Polyphenols from Nerone gold 26/6, a new pigmented rice, via non-conventional extractions: antioxidant properties and biological validation, J. Chem. Technol. Biotechnol. 96 (2021) 1691–1699, https://doi.org/10.1002/jctb.6694.
[18] A.A. Casazza, M. Capraro, M. Pedrazzi, G. D'Agostino, F. Onofri, A. Marte, R. De Tullio, P. Perego, M. Averna, Temperature-dependent olive pomace extraction for obtaining bioactive compounds preventing the death of murine cortical neurons, Int. J. Mol. Sci. 25 (2024) 907, https://doi.org/10.3390/ijms25020907.
[19] L.R. Versteegden, H.R. Hoogenkamp, R.M. Lomme, H. van Goor, D.M. Tiemessen, P.J. Geutjes, E. Oosterwijk, W.F. Feitz, T.G. Hafmans, N. Verdonschot, W. F. Daamen, T.H. van Kuppevelt, Design of an elasticized collagen scaffold: a method to induce elasticity in a rigid protein, Acta Biomater. 44 (2016) 277–285, https://doi.org/10.1016/j.actbio.2016.08.038.
[20] R. Miranda, D. Bustos-Martinez, C.S. Blanco, M.H.G. Villarreal, M.E.R. Cantú, Pyrolysis of sweet orange (Citrus sinensis) dry peel, J. Anal. Appl. Pyrolysis 86 (2009) 245–251, https://doi.org/10.1016/j.jaap.2009.06.001.
[21] A. Selvarajoo, Y.L. Wong, K.S. Khoo, W.-H. Chen, P.L. Show, Biochar production via pyrolysis of citrus peel fruit waste as a potential usage as solid biofuel, Chemosphere 294 (2022) 133671, https://doi.org/10.1016/j.chemosphere.2022.133671.
[22] P. Premchand, F. Demichelis, D. Chiaramonti, S. Bensaid, D. Fino, Study on the effects of carbon dioxide atmosphere on the production of biochar derived from slow pyrolysis of organic agro-urban waste, Waste Manag. 172 (2023) 308–319, https://doi.org/10.1016/j.wasman.2023.10.035.
[23] L. Aguiar, F. Márquez-Montesinos, A. Gonzalo, J.L. Sánchez, J. Arauzo, Influence of temperature and particle size on the fixed bed pyrolysis of orange peel residues, J. Anal. Appl. Pyrolysis 83 (2008) 124–130, https://doi.org/10.1016/j.jaap.2008.06.009.
[24] A.V. Lindner, D. Pleissner, Removal of phenolic compounds from olive mill wastewater by microalgae grown under dark and light conditions, Waste Biomass Valoriz. 13 (2022) 525–534, https://doi.org/10.1007/s12649-021-01536-5.
[25] F. Di Caprio, P. Altimari, F. Pagnanelli, Integrated microalgae biomass production and olive mill wastewater biodegradation: optimization of the wastewater supply strategy, Chem. Eng. J. 349 (2018) 539–546, https://doi.org/10.1016/j.cej.2018.05.084.
[26] G. Hodaifa, M.E. Martínez, R. Órpez, S. Sánchez, Inhibitory effects of industrial olive-oil mill wastewater on biomass production of *Scenedesmus obliquus*, Ecol. Eng. 42 (2012) 30–34, https://doi.org/10.1016/j.ecoleng.2012.01.020.
[27] I. Thushari, J. Vicheanteab, D. Janjaroen, Material flow analysis and life cycle assessment of solid waste management in urban green areas Thailand, Sustain. Environ. Res. 30 (2020) 21, https://doi.org/10.1186/s42834-020-00057-5.
[28] S.S. Lam, R.K. Liew, C.K. Cheng, N. Rasit, C.K. Ooi, N.L. Ma, J.-H. Ng, W.H. Lam, C. T. Chong, H.A. Chase, Pyrolysis production of fruit peel biochar for potential use in treatment of palm oil mill effluent, J. Environ. Manag. 213 (2018) 400–408, https://doi.org/10.1016/j.jenvman.2018.02.092.
[29] G. Stella Mary, P. Sugumaran, S. Niveditha, B. Ramalakshmi, P. Ravichandran, S. Seshadri, Production, characterization and evaluation of biochar from pod (Pisum sativum), leaf (Brassica oleracea) and peel (Citrus sinensis) wastes, international journal of recycling of organic waste, Agriculture 5 (2016) 43–53, https://doi.org/10.1007/s40093-016-0116-8.
[30] A. Abdelaal, S. Pradhan, A. AlNouss, Y. Tong, T. Al-Ansari, G. McKay, H.R. Mackey, The impact of pyrolysis conditions on orange peel biochar physicochemical properties for sandy soil, Waste Manag. Res. 39 (2021) 995–1004, https://doi.org/10.1177/0734242X20978456.
[31] W. Miran, M. Nawaz, J. Jang, D.S. Lee, Conversion of orange peel waste biomass to bioelectricity using a mediator-less microbial fuel cell, Sci. Total Environ. 547 (2016) 197–205, https://doi.org/10.1016/j.scitotenv.2016.01.004.
[32] A.T. Koçer, D. Özçimen, İ. Gökalp, An experimental study on the combustion behaviours of orange peel-based solid biofuels, Biomass Convers. Biorefinery 14 (2024) 22839–22851, https://doi.org/10.1007/s13399-023-04406-3.
[33] J.R. Ayala, G. Montero, M.A. Coronado, C. García, M.A. Curiel-Alvarez, J.A. León, C.A. Sagaste, D.G. Montes, Characterization of Orange Peel waste and valorization to obtain reducing sugars, Molecules 26 (2021) 1348, https://doi.org/10.3390/molecules26051348.
[34] H. Yu, J. Wang, J. Yu, Y. Wang, R. Chi, Effects of surface modification on heavy metal adsorption performance and stability of peanut shell and its extracts of cellulose, lignin, and hemicellulose, Environ. Sci. Pollut. Res. 27 (2020) 26502–26510, https://doi.org/10.1007/s11356-020-09055-x.
[35] B. Zapata, J. Balmaseda, E. Fregoso-Israel, E. Torres-García, Thermo-kinetics study of orange peel in air, J. Therm. Anal. Calorim. 98 (2009) 309–315, https://doi.org/10.1007/s10973-009-0146-9.
[36] A. Espina, S. Sanchez-Cortes, Z. Jurašeková, Vibrational study (Raman, SERS, and IR) of plant gallnut polyphenols related to the fabrication of Iron gall inks, Molecules 27 (2022) 279, https://doi.org/10.3390/molecules27010279.
[37] H. Yang, R. Yan, H. Chen, D.H. Lee, C. Zheng, Characteristics of hemicellulose, cellulose and lignin pyrolysis, Fuel 86 (2007) 1781–1788, https://doi.org/10.1016/j.fuel.2006.12.013.
[38] S. Dey, S.R. Basha, G.V. Babu, T. Nagendra, Characteristic and biosorption capacities of orange peels biosorbents for removal of ammonia and nitrate from contaminated water, Cleaner Mater. 1 (2021) 100001, https://doi.org/10.1016/j.clema.2021.100001.
[39] S. Giraldo, N.Y. Acelas, R. Ocampo-Pérez, E. Padilla-Ortega, E. Flórez, C.A. Franco, F.B. Cortés, A. Forgionny, Application of orange peel waste as adsorbent for methylene blue and Cd2+ simultaneous remediation, Molecules 27 (2022) 5105, https://doi.org/10.3390/molecules27165105.
[40] S.-E. Ban, E.-J. Lee, J. Yoon, D.-J. Lim, I.-S. Kim, J.-W. Lee, Role of cellulose and lignin on biochar characteristics and removal of diazinon from biochar with a controlled chemical composition, Ind. Crop. Prod. 200 (2023) 116913, https://doi.org/10.1016/j.indcrop.2023.116913.
[41] L. Luo, C. Xu, Z. Chen, S. Zhang, Properties of biomass-derived biochars: combined effects of operating conditions and biomass types, Bioresour. Technol. 192 (2015) 83–89, https://doi.org/10.1016/j.biortech.2015.05.054.
[42] Q. Abbas, G. Liu, B. Yousaf, M.U. Ali, H. Ullah, M.A.M. Munir, R. Liu, Contrasting effects of operating conditions and biomass particle size on bulk characteristics and surface chemistry of rice husk derived-biochars, J. Anal. Appl. Pyrolysis 134 (2018) 281–292, https://doi.org/10.1016/j.jaap.2018.06.018.
[43] A. Demirbas, Effects of temperature and particle size on bio-char yield from pyrolysis of agricultural residues, J. Anal. Appl. Pyrolysis 72 (2004) 243–248, https://doi.org/10.1016/j.jaap.2004.07.003.
[44] H. Haykiri-Acma, The role of particle size in the non-isothermal pyrolysis of hazelnut shell, J. Anal. Appl. Pyrolysis 75 (2006) 211–216, https://doi.org/10.1016/j.jaap.2005.06.002.
[45] H.N. Tran, S.-J. You, H.-P. Chao, Effect of pyrolysis temperatures and times on the adsorption of cadmium onto orange peel derived biochar, Waste Manag. Res. 34 (2016) 129–138, https://doi.org/10.1177/0734242X15615698.
[46] T.A. Sial, Z. Lan, M.N. Khan, Y. Zhao, F. Kumbhar, J. Liu, A. Zhang, R.L. Hill, A. H. Lahori, M. Memon, Evaluation of orange peel waste and its biochar on greenhouse gas emissions and soil biochemical properties within a loess soil, Waste Manag. 87 (2019) 125–134, https://doi.org/10.1016/j.wasman.2019.01.042.
[47] A.G. Adeniyi, J.O. Ighalo, D.V. Onifade, Biochar from the thermochemical conversion of orange (Citrus sinensis) peel and albedo: product quality and potential applications, chemistry, Africa 3 (2020) 439–448, https://doi.org/10.1007/s42250-020-00119-6.

[48] L. Pérez, J.L. Salgueiro, R. Maceiras, Á. Cancela, Á. Sánchez, Study of influence of pH and salinity on combined flocculation of Chaetoceros gracilis microalgae, Chem. Eng. J. 286 (2016) 106–113, https://doi.org/10.1016/j.cej.2015.10.059.
[49] N. Akhtar, Removal and recovery of nickel(II) from aqueous solution by loofa sponge-immobilized biomass of Chlorella sorokiniana: characterization studies, J. Hazard. Mater. 108 (2004) 85–94, https://doi.org/10.1016/j.jhazmat.2004.01.002.
[50] N. Akhtar, M. Iqbal, S.I. Zafar, J. Iqbal, Biosorption characteristics of unicellular green alga Chlorella sorokiniana immobilized in loofa sponge for removal of Cr (III), J. Environ. Sci. 20 (2008) 231–239, https://doi.org/10.1016/S1001-0742(08)60036-4.
[51] N. Akhtar, J. Iqbal, M. Iqbal, Enhancement of Lead(II) biosorption by microalgal biomass immobilized onto loofa (Luffa cylindrica) sponge, Eng. Life Sci. 4 (2004) 171–178, https://doi.org/10.1002/elsc.200420019.
[52] S. Zhang, J. Wang, Removal of chlortetracycline from water by immobilized Bacillus subtilis on honeysuckle residue–derived biochar, Water Air Soil Pollut. 232 (2021) 236, https://doi.org/10.1007/s11270-021-05193-1.
[53] S. Rossi, D. Carecci, L. Proietti, K. Parati, E. Ficara, Enhancing the environmental and economic sustainability of heterotrophic microalgae cultivation: kinetic modelling and screening of alternative carbon sources, Chem. Eng. J. Adv. 19 (2024) 100632, https://doi.org/10.1016/j.ceja.2024.100632.
[54] G. Bleve, C. Lezzi, M.A. Chiriatti, I. D'Ostuni, M. Tristezza, D.D. Venere, L. Sergio, G. Mita, F. Grieco, Selection of non-conventional yeasts and their use in immobilized form for the bioremediation of olive oil mill wastewaters, Bioresour. Technol. 102 (2011) 982–989, https://doi.org/10.1016/j.biortech.2010.09.059.
[55] M. Neifar, A. Jaouani, M.J. Martínez, M.J. Penninckx, Comparative study of olive oil mill wastewater treatment using free and immobilized Coriolopsis polyzona and Pycnoporus coccineus, J. Microbiol. 50 (2012) 746–753, https://doi.org/10.1007/s12275-012-2079-4.
[56] L.M.L. Laurens, E.J. Wolfrum, Feasibility of spectroscopic characterization of algal lipids: Chemometric correlation of NIR and FTIR spectra with exogenous lipids in algal biomass, Bioenergy Res. 4 (2011) 22–35, https://doi.org/10.1007/s12155-010-9098-y.
[57] M. Vehapi, A.T. Koçer, A. Yılmaz, D. Özçimen, Investigation of the antifungal effects of algal extracts on apple-infecting fungi, Arch. Microbiol. 202 (2020) 455–471, https://doi.org/10.1007/s00203-019-01760-7.
[58] P. SureshKumar, J. Thomas, V. Poornima, Structural insights on bioremediation of polycyclic aromatic hydrocarbons using microalgae: a modelling-based computational study, Environ. Monit. Assess. 190 (2018) 92, https://doi.org/10.1007/s10661-017-6459-4.
[59] M. Karonen, Insights into polyphenol–lipid interactions: chemical methods, molecular aspects and their effects on membrane structures, Plants 11 (2022) 1809, https://doi.org/10.3390/plants11141809.
[60] I. Kubovský, D. Kačíková, F. Kačík, Structural changes of oak wood Main components caused by thermal modification, Polymers 12 (2020) 485, https://doi.org/10.3390/polym12020485.
[61] U. Ghani, W. Jiang, K. Hina, A. Idrees, M. Iqbal, M. Ibrahim, R. Saeed, M.K. Irshad, I. Aslam, Adsorption of methyl Orange and Cr (VI) onto poultry manure-derived biochar from aqueous solution, Front. Environ. Sci. 10 (2022) 887425, https://doi.org/10.3389/fenvs.2022.887425.
[62] S. Gupta, P. Mondal, V.B. Borugadda, A.K. Dalai, Advances in upgradation of pyrolysis bio-oil and biochar towards improvement in bio-refinery economics: a comprehensive review, Environ. Technol. Innov. 21 (2021) 101276, https://doi.org/10.1016/j.eti.2020.101276.
[63] M.P. Brady, J.R. Keiser, D.N. Leonard, A.H. Zacher, K.J. Bryden, G.D. Weatherbee, Corrosion of stainless steels in the riser during co-processing of bio-oils in a fluid catalytic cracking pilot plant, Fuel Process. Technol. 159 (2017) 187–199, https://doi.org/10.1016/j.fuproc.2017.01.041.
[64] G. Manthos, D. Zagklis, C. Zafiri, M. Kornaros, Comparative life cycle assessment of anaerobic digestion, lagoon evaporation, and direct land application of olive mill wastewater, Bioresour. Technol. 388 (2023) 129778, https://doi.org/10.1016/j.biortech.2023.129778.
[65] W. Gwenzi, N. Chaukura, C. Noubactep, F.N.D. Mukome, Biochar-based water treatment systems as a potential low-cost and sustainable technology for clean water provision, J. Environ. Manag. 197 (2017) 732–749, https://doi.org/10.1016/j.jenvman.2017.03.087.
[66] O.G. Apul, T. Karanfil, Adsorption of synthetic organic contaminants by carbon nanotubes: a critical review, Water Res. 68 (2015) 34–55, https://doi.org/10.1016/j.watres.2014.09.032.
[67] W. Gwenzi, N. Chaukura, F.N.D. Mukome, S. Machado, B. Nyamasoka, Biochar production and applications in sub-Saharan Africa: opportunities, constraints, risks and uncertainties, J. Environ. Manag. 150 (2015) 250–261, https://doi.org/10.1016/j.jenvman.2014.11.027.